Domains in the 1α Dynein Heavy Chain Required for Inner Arm Assembly and Flagellar Motility in *Chlamydomonas*

Steven H. Myster,* Julie A. Knott,* Katrina M. Wysocki,* Eileen O'Toole,‡ and Mary E. Porter*

*Department of Genetics, Cell Biology, and Development, University of Minnesota Medical School, Minneapolis, Minnesota 55455; and ‡Department of Molecular, Cellular, and Developmental Biology, University of Colorado at Boulder, Boulder, Colorado 80309-0347

Abstract. Flagellar motility is generated by the activity of multiple dynein motors, but the specific role of each dynein heavy chain (Dhc) is largely unknown, and the mechanism by which the different Dhcs are targeted to their unique locations is also poorly understood. We report here the complete nucleotide sequence of the *Chlamydomonas Dhc1* gene and the corresponding deduced amino acid sequence of the 1α Dhc of the I1 inner dynein arm. The 1α Dhc is similar to other axonemal Dhcs, but two additional phosphate binding motifs (P-loops) have been identified in the NH_2- and COOH-terminal regions. Because mutations in *Dhc1* result in motility defects and loss of the I1 inner arm, a series of *Dhc1* transgenes were used to rescue the mutant phenotypes. Motile cotransformants that express either full-length or truncated 1α Dhcs were recovered. The truncated 1α Dhc fragments lacked the dynein motor domain, but still assembled with the 1β Dhc and other I1 subunits into partially functional complexes at the correct axoneme location. Analysis of the transformants has identified the site of the 1α motor domain in the I1 structure and further revealed the role of the 1α Dhc in flagellar motility and phototactic behavior.

Key words: motors • dynein • flagella • phototaxis • inner arm

THE movement of cilia and flagella is powered by axonemal dyneins, a family of mechanoenzymes that convert the energy derived from ATP binding and hydrolysis into the sliding of adjacent outer doublet microtubules (Mitchell, 1994; Witman et al., 1994; Porter, 1996). Axonemal dyneins can be separated into two groups, the outer dynein arms and the inner dynein arms, which have different functions in generating and propagating the flagellar waveforms. The outer dynein arms provide power to the flagellar beat, as *Chlamydomonas* mutants lacking the outer arms generate normal waveforms, but swim with a reduced beat frequency (Mitchell and Rosenbaum, 1985; Brokaw and Kamiya, 1987). In contrast, the inner arms are essential for normal motility, as mutants with inner arm defects have near normal beat frequencies, but display aberrant waveforms (Brokaw and Kamiya, 1987).

The *Chlamydomonas* outer arm is one of the most well characterized dynein complexes; it is composed of three dynein heavy chains (Dhc)[1] (α, β, and γ), two intermediate chains (IC), and several light chains (LCs) (<20 kD), and repeats every 24 nm along the length of the axoneme (Witman et al., 1994). Sequence comparisons between outer arm Dhcs indicate that they share greatest similarity in the central and COOH-terminal regions (Mitchell and Brown, 1994, 1997; Wilkerson et al., 1994; Gibbons, 1995). This portion of the Dhc is thought to form a globular head domain that interacts transiently with the microtubule doublet during the cross-bridge cycle. The more variable NH_2-terminal third of the Dhc is thought to form a flexible stem domain that extends to the base of the dynein arm and interacts with the isoform-specific IC and LC subunits (Sakakibara et al., 1993). The ICs are involved in the assembly of the outer arm complex (Mitchell and Rosenbaum, 1986; Mitchell and Kang, 1991) and its attachment to the outer doublet microtubules in an ATP-insensitive manner (S.M. King et al., 1991, 1995). The multiple LCs are thought to be involved in the regulation of motility, but their specific functions are largely unknown (Harrison and King, 1999).

The inner dynein arms share an overall structural similarity to the outer arms but are significantly more complex

Address correspondence to Mary E. Porter, Department of Genetics, Cell Biology, and Development, University of Minnesota Medical School, Box 206, 420 Delaware St. SE, 4-102 Owre Hall, Minneapolis, MN 55455. Tel.: (612) 626-1901. Fax: (612) 624-8118. E-mail: mary-p@biosci.cbs.umn.edu

Abbreviations used in this report: BAC, bacterial artificial chromosome; Dhc, dynein heavy chain; IC, intermediate chain; LC, light chain; OA, outer arm; P-loop, phosphate binding motif; P1-P4, Pn, Pc, P-loops 1-4, NH_2- and COOH-terminal P-loop; RT-PCR, reverse transcriptase PCR.

in both composition and function. Ion exchange chromatography and SDS-PAGE procedures have identified at least eight distinct inner arm Dhcs that are associated with specific ICs and LCs into seven different molecular complexes: one two-headed isoform (I1) and six single-headed isoforms (I2 and I3) (Goodenough et al., 1987; Kagami and Kamiya, 1992). These isoforms are arranged in complex groups along the length of the axoneme (Piperno et al., 1990; Piperno and Ramanis, 1991; Muto et al., 1991; Mastronarde et al., 1992; Gardner et al., 1994; S.J. King et al., 1994), but the relationship between these different isoforms and the multiple *Dhc* genes (Porter et al., 1996, 1999) is almost completely unknown.

Very little is also understood about the mechanism by which any Dhc is targeted to its specific location within the axoneme. In this report, we focus on the role of the 1α Dhc in the assembly and targeting of the inner arm isoform known as the I1 complex. The I1 dynein provides several advantages for the study of dynein targeting. First, it is a relatively simple complex composed of two Dhcs (1α and 1β), three ICs of 140, 138, and 110 kD (Piperno et al., 1990; Smith and Sale, 1991; Porter et al., 1992) and three LCs of 14, 12, and 8 kD (Harrison et al., 1998). Second, the I1 complex has a well-defined axoneme location, proximal to the first radial spoke in each 96-nm repeat along the length of the axoneme (Piperno et al., 1990; Mastronarde et al., 1992; Porter et al., 1992; Myster et al., 1997). Third, the I1 complex is an important target for the regulation of flagellar motility (Porter et al., 1992). Alterations in the phosphorylation state of IC138 have been associated with changes in microtubule sliding velocities and phototactic behavior (Habermacher and Sale, 1997; King and Dutcher, 1997). Finally, progress in the cloning and mapping of *Dhc* genes has identified two sequences that encode the I1 Dhcs (Porter et al., 1996; Myster et al., 1997; Perrone, C.A., R. Bower, S.H. Myster, J.A. Knott, and M.E. Porter, unpublished results). One of these sequences, *Dhc1*, maps to the *PF9*/*IDA1* locus and encodes the 1α Dhc; mutations in this locus disrupt the assembly of the I1 complex and thereby alter flagellar motility (Myster et al., 1997). The availability of such mutations permits a functional analysis of the *Dhc1* gene product in vivo.

To characterize the Dhc domains involved in the assembly and targeting of the I1 complex, we sequenced the complete *Dhc1* transcription unit (>22 kb) and generated specific constructs of the *Dhc1* gene. The constructs were used in cotransformation experiments to rescue the *pf9* defects. These results represent the first full-length inner arm Dhc sequence to be described in any organism, and the first reported rescue of a *Dhc* mutation in *Chlamydomonas*. Our analysis of the *Dhc1* transformants has also identified a subset of strains expressing truncated *Dhc1* transcripts. The truncated transcripts encode NH_2-terminal fragments of the 1α Dhc polypeptide that are capable of coassembly with other components of the I1 complex and rebinding to the proper axoneme location. These results indicate that domains within the NH_2-terminal ~143 kD of the 1α Dhc are involved in the specific subunit interactions required for the assembly and targeting of the I1 complex. EM analysis of isolated axonemes has identified the position of the 1α Dhc motor domain within the structure of the I1 complex. The assembly of truncated 1α Dhcs in the flagella of the transformants also resulted in a new motility phenotype that has revealed the contribution of the 1α Dhc motor domain to flagellar motility and phototactic behavior. These findings have important implications for the regulatory mechanisms that control the activity of the I1 dynein motor.

Materials and Methods

Origin of Genomic Clones and Sequence Analysis of the Dhc1 Gene

35 kb of genomic DNA in the region of the *Dhc1* gene was recovered from a large insert, wild-type (21gr) *Chlamydomonas* library. The position of the *Dhc1* transcription unit within this region was determined by probing Northern blots of wild-type RNA with selected subclones, and the *Dhc1* transcription unit was thereby narrowed down to ~22 kb of genomic DNA (see Fig. 1; Myster et al., 1997). Sequence information was obtained from both strands of subclones A–D, and G using a series of nested deletions (Erase-a-Base System; Promega Corp.) and Sequenase 2.0 (Amersham Life Science, Inc.) following the manufacturer's instructions. Subclones E and F were sequenced by the DNA Sequencing Facility (Iowa State University) on an ABI Prism sequencer (Perkin Elmer Corp.). The sequence data were assembled using the GCG software package versions 8 and 9 (Genetics Computer Group).

Potential open reading frames were identified using the GCG program CodonPreference and a codon usage table compiled from the coding regions of 73 different *Chlamydomonas* nuclear sequences (Nakamura et al., 1997; available at http://www.dna.affrc.go.jp/~nakamura/codon.html). Potential splice donor and acceptor sequences within the open reading frames were identified based on splice junction consensus sequences found in *Chlamydomonas* nuclear genes (Mitchell and Brown, 1994; LeDizet and Piperno, 1995; Zhang, 1996; R. Schnell, personal communication).

In five regions of the *Dhc1* gene, the presence of multiple potential splice donor or acceptor sequences did not allow a confident prediction of the putative exons. In those cases, the splice junctions were determined directly by sequence analysis of reverse transcriptase–PCR (RT-PCR) products generated from the *Dhc1* transcript (see Fig. 1). Total RNA was isolated from wild-type cells 45 min after deflagellation, and then 5 μg of total RNA was reverse transcribed using either a random primer or a sequence-specific reverse primer and the Superscript Preamplification System (GIBCO BRL) according to manufacturer's instructions. 5 μl of the resulting 25-μl cDNA product was used in a 100-μl PCR reaction with sequence specific primers. PCR reactions were performed using 20 mM Tris-HCl, pH 8.4, 50 mM KCl, 1.5 mM $MgCl_2$, 2 mM deoxynucleotide triphosphates, 0.2 mM of each primer, and 2.5 U *Taq* polymerase (Life Technologies, Inc.). Some reactions also contained 3% DMSO. The PCR reactions were first denatured at 94°C for 3 min, followed by 30 cycles of 58°C for 1 min, 72°C for 3 min, and 94°C for 1 min, and then completed with a final cycle of 58°C for 1 min and 72°C for 5 min. The final reaction products were analyzed on agarose gels, and then purified using Wizard PCR preps (Promega Corp.) for direct sequencing with sequence-specific primers.

The proposed translation start site was determined by the recovery of an RT-PCR product using a forward primer downstream of the TATA box sequence and a reverse primer in exon 3. The resulting RT-PCR product contained stop codons in all three frames immediately preceding the proposed start codon.

The predicted amino acid sequence encoded by the *Dhc1* gene was analyzed using the GCG program Motifs. The programs Bestfit, Compare, and Pileup were used to compare the 1α Dhc sequence to *Chlamydomonas* outer arm Dhc sequences α, β, and γ (Mitchell and Brown 1994, 1997; Wilkerson et al., 1994) and the cytoplasmic Dhc from *Dictyostelium* (Koonce et al., 1992). Regions with the potential to form α-helical coiled coils were identified using the program COILS, version 2.2 (Lupus et al., 1991; Lupus, 1996).

Cosmid Library Screening and Construction of pD1SA

To identify clones that might contain a full-length *Dhc1* gene, we screened two different *Chlamydomonas* cosmid libraries (Purton and Rochaix, 1994; H. Zhang et al., 1994) that were generously provided by S. Purton

(University College, London) and D. Weeks (University of Nebraska). Because the Purton library contains the *ARG7* gene within the cloning vector, the cosmid clones can be used to directly transform *arg7* strains. 10^5 independent clones from each library were screened on Magnagraph (Micron Separations, Inc.) nylon membrane lifts in duplicate with probes from the 5′ and 3′ ends of the *Dhc1* gene (see Fig. 5 A). Probes used for hybridization were purified in low melting point agarose (GIBCO BRL) and radiolabeled with [^{32}P]dCTP and random hexamer primers using the Prime It II kit (Stratagene). Conditions for prehybridization and hybridization were as described previously (Porter et al., 1996; 1999; Myster et al., 1997). After single colony isolation, cosmid DNA was purified using alkaline lysis procedures and CsCl gradient centrifugation (Sambrook et al., 1989).

A truncated version of the *Dhc1* gene was constructed by fusing sequences from the 5′ end to sequences from the 3′ end. To recover the 5′ end, a 19-kb SalI fragment was subcloned to form the plasmid pSM8 (see Fig. 5 D). pSM8 contains ~1.7 kb of genomic DNA located 5′ of the coding region, but ends in the middle of the *Dhc1* transcription unit. pSM8 was digested with SalI and AscI to release the *Dhc1* gene as an 11-kb fragment that is truncated before the region encoding the ATP hydrolytic site (P1). The 3′ end of the *Dhc1* gene was subcloned as a 4.3-kb SalI, EcoRI fragment to form the plasmid p14SE, which was digested with SalI and AscI to release the region 5′ of the AscI site. The SalI-AscI fragment from pSM8 was ligated into the digested p14SE subclone to form the construct pD1SA (see Fig. 5 D). pD1SA joins sequences from the 5′ end of the *Dhc1* gene to the 3′ end at the AscI site. It is predicted to encode the first 1,956 amino acids of the 1α Dhc, and then terminate translation after adding nine novel amino acids (QCHGCGPGV) to the COOH terminus of the polypeptide.

Recovery of Bacterial Artificial Chromosome (BAC) Clones Containing the Dhc1 Gene

A modified pBELO BAC library containing *Chlamydomonas* genomic DNA was screened with selected subclones to identify large insert BAC clones containing the *Dhc1* gene. This library was constructed by N. Haas and P. Lefebvre (University of Minnesota, St. Paul, MN) using genomic DNA from the cell-wall less strain cw92 and is currently available from Genome Systems, Inc. BAC DNA was isolated from positive clones using a modified version of the manufacturer's protocol available from C. Amundsen (University of Minnesota, St. Paul, MN) at the following URL: http://biosci.cbs.umn.edu/~amundsen/chlamy/methods/bac.html. The final pellet of BAC DNA was resuspended in 200 μl of TE and stored at −20°C. To identify clones containing full-length *Dhc1* genes, 5 μl of BAC DNA was digested with the restriction enzyme SacI and analyzed on Southern blots using subclones from the 5′ and 3′ ends of the *Dhc1* gene.

Nucleic Acid Analysis

Large-scale preparations of genomic DNA were isolated from wild-type and mutant transformant strains using CsCl gradients as described in Porter et al. (1996). A smaller scale mini-prep procedure (Newman et al., 1990) was used to isolate DNA samples from tetrad progeny and some of the transformants. Restriction enzyme digests, agarose gels, isolation of total RNA, and Southern and Northern blots were performed as previously described (Porter et al., 1996, 1999; Myster et al., 1997).

Cell Culture, Mutant Strains, and Cotransformation Experiments

The strains used in this study are listed in Table I. All cells were maintained as vegetatively growing cultures at 21°C as previously described (Myster et al., 1997). The *arg2* (Eversole, 1956) strains were grown on rich medium that contained reduced ammonium nitrate (one tenth the normal concentration), but was supplemented with L-arginine to 0.6 mg/ml.

The *pf9-2 arg2* strain (Porter et al., 1992) was crossed to the outer arm mutant *pf28* using standard genetic techniques (Levine and Ebersold, 1960; Harris, 1989) to obtain the triple mutant *pf9-2 pf28 arg2*. The *pf9-2 pf28 arg2* strain assembles short, immotile flagella, and requires arginine for growth. After growth in tris-acetate phosphate (TAP) media supplemented with 0.6 mg/ml L-arginine, this strain was cotransformed using the glass bead method (Kindle, 1990; Nelson et al., 1994) with various constructs of the *Dhc1* gene (2–4 μg) and the plasmid pARG7.8, which contains a wild-type copy of the *ARG7* (argininosuccinate lyase) gene (Debuchy et al., 1989). After transformation, cells were washed and plated on TAP media lacking arginine to select for arg+ transformants. After 10 d of growth, single arg+ colonies were picked into liquid media and tested for rescue of the flagellar assembly and motility defects.

Analysis of Motility

Positive transformants were picked into 96-well plates and screened for motility on an inverted microscope (Olympus CK). Wells containing motile cells were streaked for single colonies and rescored on a phase-contrast microscope (Axioskop; Carl Zeiss, Inc.) using a 40× objective and a 10× eyepiece. The phenotypes of motile transformants were further analyzed by measuring forward swimming velocities and beat frequencies as previously described (Porter et al., 1992, 1994; Myster et al., 1997).

Transformants were tested for their ability to phototax using two different assays. In the first assay (King and Dutcher, 1997), actively swimming cells were put in a dark box with a 3-cm-wide horizontal slit cut out along the bottom such that only the lower portion of a 10-ml suspension was illuminated. The box was placed ~35 cm from a fluorescent light source for 40 min. Positively phototactic cells would concentrate in the lower, illuminated portion of the tube, whereas phototaxis defective cells would remain uniformly suspended throughout the tube. In the second assay, motile cells were transferred to a 96-well plate and placed on a dissecting microscope with substage illumination. Thick posterboard was placed under the plate and positioned to cover half of the well. The location of the cells within the well was followed over a 60-min time course. Positively phototactic cells would move quickly to the side of the well exposed to light, whereas cells unable to phototax would remain uniformly distributed throughout the well.

To verify that the rescued motility in the transformants was due to expression of the *Dhc1* transgene and not a reversion event at the *PF9* locus, the motile transformants were backcrossed to a *pf28* allele (*oda2*), which lacks the outer arms but is wild-type at the *PF9* locus (Kamiya, 1988). Tetrad progeny were recovered following standard genetic methods (Harris, 1989), and their motility phenotypes were scored using a phase-contrast microscope as described above.

Axoneme Isolation, Dynein Extracts, and Sucrose Gradients

Axonemes were prepared from large-scale (5–40 liters) liquid cultures of vegetative cells using procedures described by Witman (1986) and S.M. King et al. (1986), as modified by Gardner et al. (1994) and Myster et al. (1997). Crude dynein extracts were obtained by brief (~30 min) high salt extraction of whole axonemes (Porter et al., 1992; Myster et al., 1997). To isolate I1 complexes, crude dynein extracts were fractionated by sucrose density gradient centrifugation as previously described (Porter et al., 1992; Myster et al., 1997). Aliquots of each fraction were analyzed by SDS-PAGE and Western blotting.

SDS-PAGE and Immunoblot Analysis

Protein samples from whole axonemes and sucrose gradient fractions were separated on 5% polyacrylamide gels using the Laemmli (1970) buffer system and either stained directly with Coomassie brilliant blue (R250; Sigma Chemical Co.) or transferred to either nitrocellulose (Schleicher and Schull, Keene) or Immobilon-P (Millipore) in 25 mM Tris, 192 mM glycine, and 12.5% methanol at 800 mA for 90 min at 4°C using a Genie electroblotter (Idea Scientific, Co.). Nitrocellulose blots were blocked in 1× PBS (0.58 M Na_2HPO_4, 0.017 M $NaH_2PO_4 \cdot H_2O$, 0.68 M NaCl), 5% normal goat serum (Sigma Chemical Co.), and 0.05% Tween 20 (polyethylenesorbitan monolaurate), whereas the Immobilon-P membrane was blocked in 0.2% I-Block (Tropix) in 1× PBS and 0.5% Tween 20.

Four different antibody preparations were used to probe the blots. The 1α Dhc antibody has been previously described in detail and is highly specific for the *Dhc1* gene product (Myster et al., 1997). This antibody was raised against the peptide sequence DGTCVETPEQRGATD, which corresponds to amino acids 1,059–1,073 of the 1α Dhc polypeptide. The 1α Dhc antibody was affinity-purified on Western blots of dynein extracts, and then used at a 1:10 dilution. The IC140 antibody was provided by P. Yang and W. Sale (Emory University, Atlanta, GA). This antiserum was raised against a fusion protein containing a fragment of the 140-kD intermediate chain of the I1 complex (Yang and Sale, 1998), and it was typically used at a dilution of 1:3,000. The rabbit polyclonal antibody R5205, which was raised against a fusion protein of the human 14-kD dynein LC (S.M. King et al., 1996), was provided by S. King (University of Connecti-

Table I. Strains Used in this Study

Strain name	Dynein defect	Swimming phenotype	Reference
Wild-type (137c)	None	Wild-type	Harris, 1989
pf9-2	I1 complex	Slow, smooth swimming	Porter et al., 1992
pf9-2 arg2	I1 complex	Slow, smooth swimming	Porter et al., 1992
pf28	Outer arm	Slow, jerky swimming	Mitchell and Rosenbaum, 1985
oda2	Outer arm	Slow, jerky swimming	Kamiya, 1988
pf9-2 pf28 arg2	Outer arm & I1 complex	Short, paralyzed flagella	This study
cW1 cotransformants			
C1	Outer arm, partial I1	Slow, jerky swimming	This study
E2	Outer arm, partial I1	Slow, jerky swimming	This study
F2	Outer arm, partial I1	Slow, jerky swimming	This study
F3	Outer arm, partial I1	Slow, jerky swimming	This study
F4	Outer arm, partial I1	Slow, jerky swimming	This study
F5	Outer arm, partial I1	Slow, jerky swimming	This study
F7	Outer arm, partial I1	Slow, jerky swimming	This study
G3	Outer arm, partial I1	Slow, jerky swimming	This study
G4	Outer arm, partial I1	Slow, jerky swimming	This study
G9	Outer arm, partial I1	Slow, jerky swimming	This study
G11	Outer arm, partial I1	Slow, jerky swimming	This study
cA1 cotransformants			
A2	Outer arm, partial I1	Slow, jerky swimming	This study
A3	Outer arm, partial I1	Slow, jerky swimming	This study
A4	Outer arm, partial I1	Slow, jerky swimming	This study
A5	Outer arm, partial I1	Slow, jerky swimming	This study
pD1SA cotransformants			
H1	Outer arm, partial I1	Slow, jerky swimming	This study
H2	Outer arm, partial I1	Slow, jerky swimming	This study
H3	Outer arm, partial I1	Slow, jerky swimming	This study
H4	Outer arm, partial I1	Slow, jerky swimming	This study
H5	Outer arm, partial I1	Slow, jerky swimming	This study
H6	Outer arm, partial I1	Slow, jerky swimming	This study
H10	Outer arm, partial I1	Slow, jerky swimming	This study
BAC cotransformants			
2A-1B	Outer arm	Slow, jerky swimming	This study
2B-4E	Outer arm	Slow, jerky swimming	This study
4B-C2	Outer arm	Slow, jerky swimming	This study
4B-G2	Outer arm	Slow, jerky swimming	This study
5B-G10	Outer arm	Slow, jerky swimming	This study
Dhc1 deletion strains			
pf9-3	I1 complex	Slow, smooth swimming	Myster et al., 1997
E2+OA	Partial I1	Fast swimming	This study
G4+OA	Partial I1	Fast swimming	This study

cut). The R5205 antibody cross-reacts with the 14-kD LC (Tctex1) of the I1 complex (Harrison et al., 1998) and was used at a dilution of 1:50. After incubation overnight at 4°C, the blots were washed in 1× PBS and 0.05% Tween 20. Immunoreactivity was detected using an alkaline phosphatase–conjugated secondary antibody, BCIP (5-bromo-4-chloro-3-indolyl phosphate), and NBT (nitro blue tetrazolium) following the manufacturer's instructions (Sigma Chemical Co.). An mAb to tubulin (T5168; Sigma Chemical Co.) was used at a dilution of 1:1,000, and then detected using an HRP-conjugated secondary antibody, 4-chloro-1-naphthol, and hydrogen peroxide following the manufacturer's protocol (Sigma Chemical Co.).

Electron Microscopy and Image Analysis

To view the I1 complex in strains with rescued motility, selected transformants were crossed to a *pf9-3* strain to recover strains with rescued I1 complexes and the wild-type complement of outer dynein arms. Axonemes were prepared and processed for EM as previously described (Porter et al., 1992; Myster et al., 1997). Longitudinal images were selected, digitized, and averaged using the methods described in Mastronarde et al. (1992). Averages of individual axonemes were obtained by analyzing at least six 96-nm radial spoke repeats, and then averages from several axonemes were combined to obtain a grand average for each strain. The methods used to compute differences between two strains are described in detail in Mastronarde et al. (1992).

Recovery of Dhc1 Transgene from G3 After Transformation

To identify the 3′ end of the *Dhc1* transgene in the G3 transformant (which assembles the shortest 1α Dhc fragment), genomic DNA was isolated from wild-type and G3, digested with the restriction enzymes SacI and KpnI, and analyzed on Southern blots probed with *Dhc1* subclones. A polymorphic 7.2-kb SacI-KpnI fragment was identified in G3 using subclone C. This polymorphic fragment was recovered from G3 genomic DNA by constructing a size-selected minilibrary, and then screening the library with subclone C. After single colony purification, the 3′ end of the truncated *Dhc1* transgene was sequenced with *Dhc1* specific primers to determine the predicted amino acid sequence at the COOH terminus of the 1α Dhc fragment.

Results

Sequence Analysis of the Dhc1 Transcription Unit

In previous work, we identified a null mutation in the *Dhc1* gene that resulted in the failure to assemble the I1 inner arm complex into the flagellar axoneme (Myster et al.,

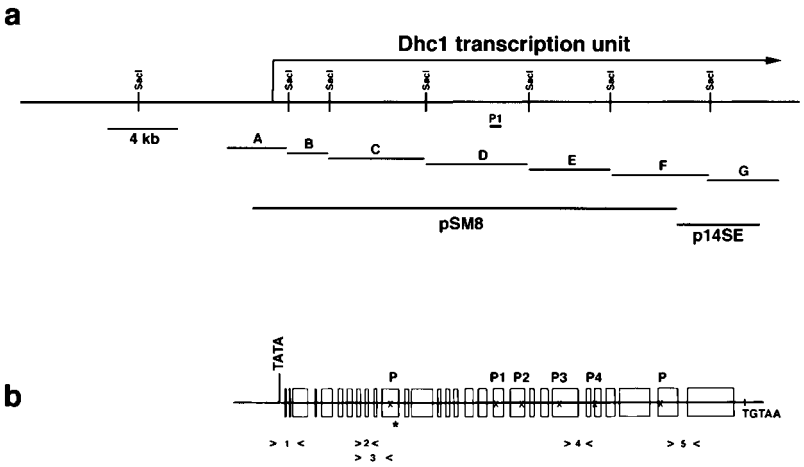

Figure 1. *Dhc1* gene structure. (a) Partial restriction map of the *Dhc1* gene. The black box labeled P1 represents the 227 bp fragment of the *Dhc1* gene that was recovered in the first PCR screen for *Dhc* genes in *Chlamydomonas* (Porter et al., 1996). This sequence was used to screen a large insert genomic library and recover >35 kb of genomic DNA surrounding the region encoding the hydrolytic ATP binding site (P1) (Porter et al., 1996; Myster et al., 1997). Indicated below are the approximate positions of selected SacI subclones (A–G) used as probes and other subclones (pSM8 and p14SE) that were used to construct a truncated *Dhc1* gene. (b) Intron/exon structure of the *Dhc1* transcription unit. The approximate size and position of the 29 exons (open boxes) and 28 introns (intervening lines) predicted from the analysis of the *Dhc1* nucleotide sequence are shown. Also indicated are other features such as the TATA box, the regions encoding predicted P-loops, and a predicted polyadenylation signal at the 3′ end of the gene. Bracketed regions numbered 1–5 indicate the position of the primers used for RT-PCR.

1997). To understand how the *Dhc1* gene product might contribute to dynein complex formation, we have now sequenced the entire *Dhc1* transcription unit (Fig 1 a). A map of the deduced gene structure is shown in Fig. 1 b. Sequence analysis of subclone A identified the 3′ end of the neighboring gene (geranyl geranyl pyrophosphate synthase), ~800 bp of intervening sequence, and a TATA box sequence 144 bp upstream of the proposed translation start site of the *Dhc1* gene (see Materials and Methods). All of the 5′ sequence elements required for regulated *Dhc1* expression should therefore be contained within an ~1-kb region. The next 20 kb of the sequence contains the coding region located within 29 exons. The 3′ end of the gene is located in subclone G, which contains the last exon encoding the COOH-terminal 552 amino acids, a stop codon, and a consensus polyadenlyation signal sequence (TGTAA) 471 bp downstream.

The predicted amino acid sequence of the encoded 1α Dhc contains 4,625 amino acid residues and corresponds to a polypeptide of 522,806 D (Fig. 2). A search for potential nucleotide binding sites within the 1α Dhc sequence identified six consensus or near consensus phosphate-binding (P-loop) motifs with the sequence A/GXXXX-GKT/S (Walker et al., 1982). Four of the P-loop motifs (P1–P4) are located within the central region of the Dhc, and both spacing and sequences of these P-loops are similar among all Dhc sequences reported thus far (reviewed in Gibbons, 1995; Porter, 1996). Two additional P-loop motifs were identified in the NH_2-terminal (Pn) and COOH-terminal (Pc) regions of the 1α Dhc respectively; these appear to be unique to the 1α Dhc (Fig. 2).

The predicted amino acid sequence of the 1α Dhc was compared with the three Dhc sequences (α, β, and γ) that form the outer dynein arm in *Chlamydomonas* (Mitchell and Brown, 1994, 1997; Wilkerson et al., 1994) and the cytoplasmic Dhc from *Dictyostelium* (Koonce et al., 1992). In each case, a high degree of sequence similarity was apparent over long stretches of the polypeptide, especially in the central and COOH-terminal thirds of the Dhc (28–38% identity, 58–67% similarity). However, the more variable NH_2-terminal third of the 1α Dhc also shares significant homology with the β and γ Dhcs of the outer arm (Fig. 3, ~24% identity, ~56% similarity). Alignment of the Dhc sequences using the GCG program PILEUP confirmed that the presence of conserved domains within the NH_2-terminal region, but also revealed several short stretches of unique peptide sequence in the 1α Dhc, including the region previously used to generate a monospecific 1α Dhc antibody (Fig. 2; Myster et al., 1997).

The 1α Dhc sequence was also analyzed using programs that predict secondary structure to identify regions with the potential to form α-helical coiled-coil domains (Lupus et al., 1991; Lupus, 1996) (Fig. 4). One region located before P-loop 1 (residues 1,227–1,409) and a second after the P-loop 4 (residues 3,192–3,297, 3,400–3,494, and 3,701–3,789) show the highest probability of forming α-helical coiled coils. The presence of limited coiled-coil domains separating the central portion of the Dhc from the NH_2-terminal and COOH-terminal regions has been observed in other Dhc sequences (Mitchell and Brown, 1994, 1997; Porter, 1996). These conserved structural domains are thought to play an important role in protein interactions within the dynein arms.

Isolation of Dhc1 Transgenes

To better understand how the specific domains of the 1α Dhc polypeptide might be involved in the assembly and activity of the I1 inner arm dynein, we decided to analyze constructs of the *Dhc1* gene in vivo in a *pf9* mutant background. Because of the large size of the *Dhc1* gene (~21 kb), two cosmid libraries and one BAC library were screened with probes representing the 5′ and 3′ ends of the *Dhc1* gene to improve the chances of recovering clones that contain the full-length gene (Fig. 5 A). The first cosmid library yielded a single clone, cA1, which was positive with both probes, but upon further analysis proved to be lacking a small portion at the 3′ end of the gene (Fig. 5 B). Screening the second cosmid library resulted in the recovery of a single clone, cW1, which contained the complete *Dhc1*

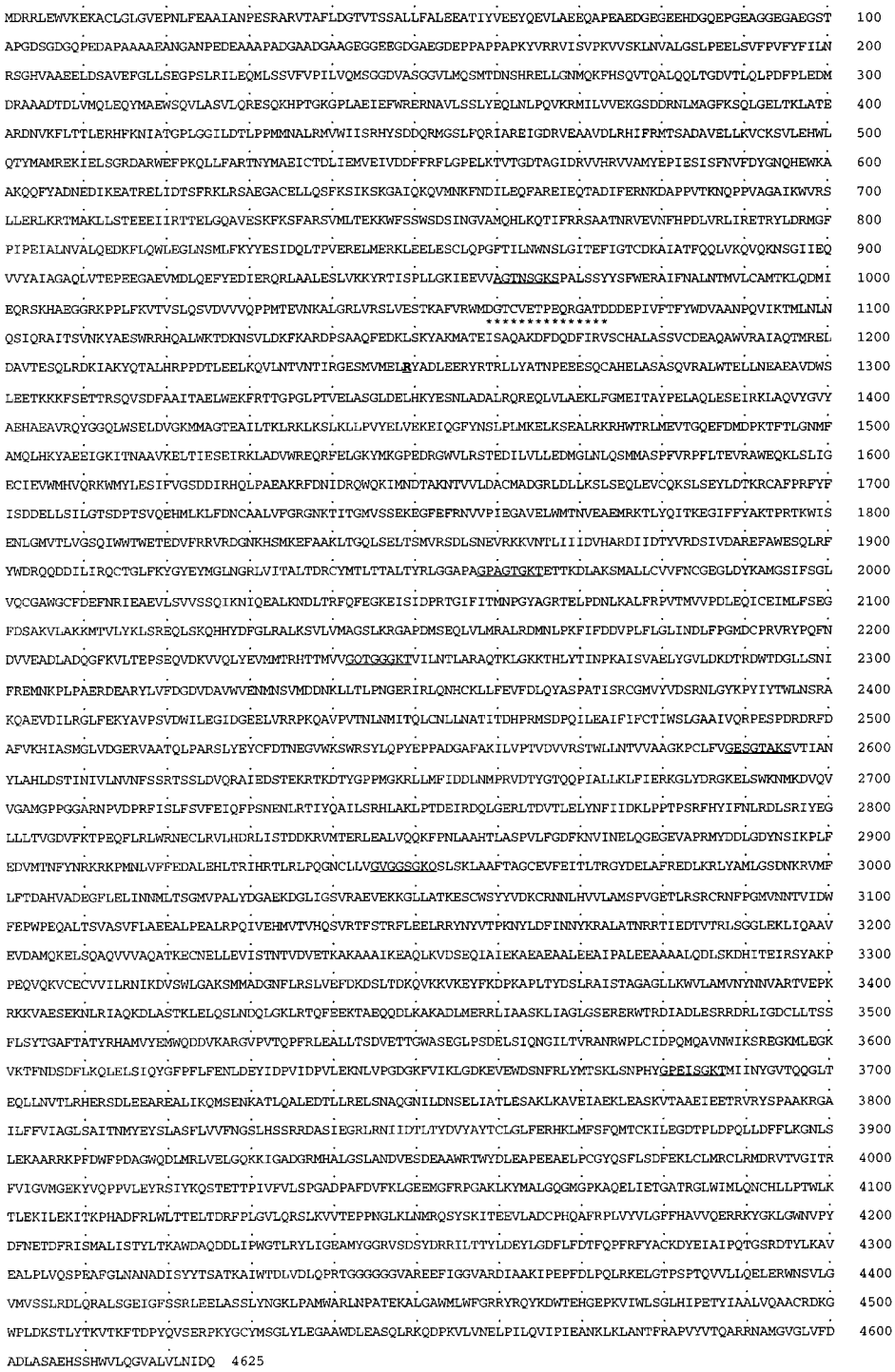

Figure 2. Predicted amino acid sequence of the 1α Dhc. Sequences identified as P-loop motifs are indicated by a single underline. The amino acid sequence of the peptide used for antibody production by Myster et al. (1997) is indicated by asterisks. The arginine (R) residue at the COOH-terminal end of the truncated 1α Dhc in the G3 transformant is indicated by bold and an underline. The complete nucleotide sequence is available from GenBank/EMBL/DDBJ under accession number AJ243806.

transcription unit as well as additional genomic sequences both 5′ and 3′ that might be required for proper expression in vivo (Fig. 5 C). Four larger clones (100–135 kb) containing the *Dhc1* transcription unit were recovered from the BAC library; two of these clones were used in subsequent cotransformation experiments (Fig. 5 E). We also constructed a truncated version of the *Dhc1* transgene known as pD1SA by fusing an 11-kb region encoding the NH_2-terminal 1,956 amino acids to a 1-kb region containing the 3′ end of the gene (Fig. 5 D). All of the *Dhc1* transgenes were tested for their ability to rescue the *pf9* mutant defects in vivo.

Rescue of pf9 Motility Defects by Transformation with Constructs of the Dhc1 Gene

Mutations at the *PF9/IDA1* locus typically result in strains that have a slow, smooth swimming behavior (Kamiya et al., 1991; Porter et al., 1992). To increase the sensitivity of the screen for rescue of the *pf9* mutant phenotype, we intro-

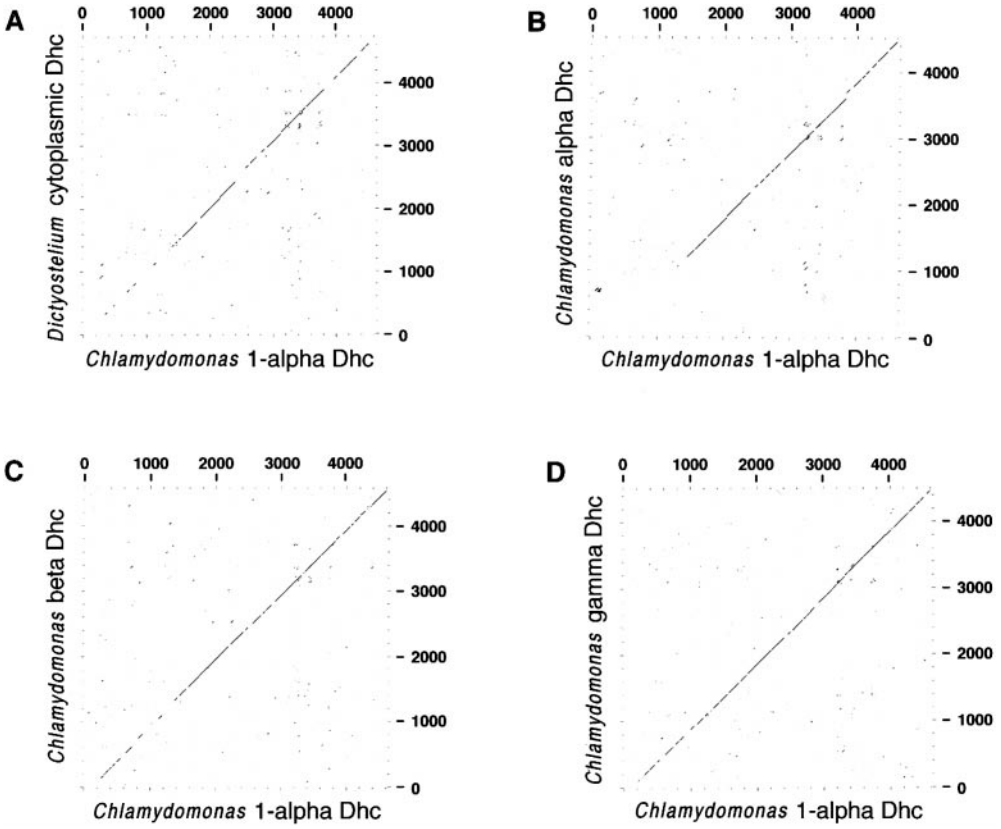

Figure 3. Comparisons between Dhc sequences. The 1α Dhc was compared with the *Chlamydomonas* outer arm Dhc sequences (α, β, and γ) and the *Dictyostelium* cytoplasmic Dhc using the GCG program COMPARE with a window of 50 residues and a stringency of 22. The accession numbers for these sequences are as follows: L26049, U02963, U15303, and Z15124.

duced a second motility mutation into the *pf9-2* background. *pf28* is a mutation in the γ Dhc gene that results in the failure to assemble the outer dynein arms (Mitchell and Rosenbaum, 1985; Wilkerson et al., 1994). Cells carrying the *pf28* mutation swim with a jerky phenotype that can be easily distinguished from the slow, smooth swimming behavior of the *pf9* mutant cells. In addition, *pf9-2 pf28* double mutants assemble short, paralyzed flagella and sink in liquid medium (Porter et al., 1992). This short, paralyzed flagellar phenotype makes it very straightforward to identify transformants that have rescued the *pf9* mutant defects by screening for cells that assemble full-length, motile flagella and swim with a *pf28*-like motility phenotype.

The *pf9-2 pf28 arg2* strain was first cotransformed with the selectable marker pARG7.8 and the cW1 cosmid containing the complete *Dhc1* transcription unit. Positive transformants were selected by growth on solid medium lacking arginine, and then single colonies were picked into liquid media and screened for motility. Fig. 5 C illustrates the combined results of several independent cotransformation experiments with the cW1 cosmid. Although arg+ transformants were recovered at expected frequencies (Kindle, 1990), only 11 out of 2,880 transformants screened displayed any motility, for a frequency of rescue of <0.4%. Moreover, the motility of the cW1 rescued strains was not the same as *pf28* (see below and Table II).

Given these preliminary findings, we decided to test the other *Dhc1* transgenes for their ability to rescue the mutant phenotypes. The cosmid cA1 contains an incomplete copy of the *Dhc1* transcription unit but also contains the *ARG7* gene cloned within the bacterial vector sequences, thereby physically linking the selectable marker and the *Dhc1* gene. Therefore, all arg+ transformants might be expected to contain the *Dhc1* sequence integrated along with the *ARG7* gene. However, the frequency of rescue with the cA1 cosmid (0.61%; Fig. 5 B) was only slightly better than the cW1 cosmid. These observations indicated the *Dhc1* transgenes were probably being fragmented during the transformation protocol, but the recovery of motile strains also suggested that a truncated version of the *Dhc1* sequence was capable of restoring some function.

Previous study of an outer arm mutation, *oda4-s7*, had indicated that the NH_2-terminal third of the β Dhc polypeptide is sufficient for assembly of a dynein complex (Sakakibara et al., 1993). To test if this is also true for the 1α Dhc, we cotransformed the *pf9 pf28* mutant with the smaller pD1SA construct, which encodes ~40% of the 1α Dhc sequence. These experiments yielded seven motile strains (Fig. 5 D), which represented only a modest (0.87%) increase in the frequency of rescue, but these rescues confirmed that truncated *Dhc1* transgenes could restore partial motility. To see if it was possible to completely rescue the motility defects, we also transformed the *pf9 pf28* mutant with two BAC clones that contained the full-length *Dhc1* gene located in the middle of ~100–135-kb genomic inserts (Fig. 5 E). The frequency of rescue (~0.1%) was still quite low, but the motility phenotypes of the rescued strains were very similar to *pf28* (see below).

The recovery of motile isolates after cotransformation could also be due to an intragenic reversion event at the *PF9* locus during the course of transformation and/or se-

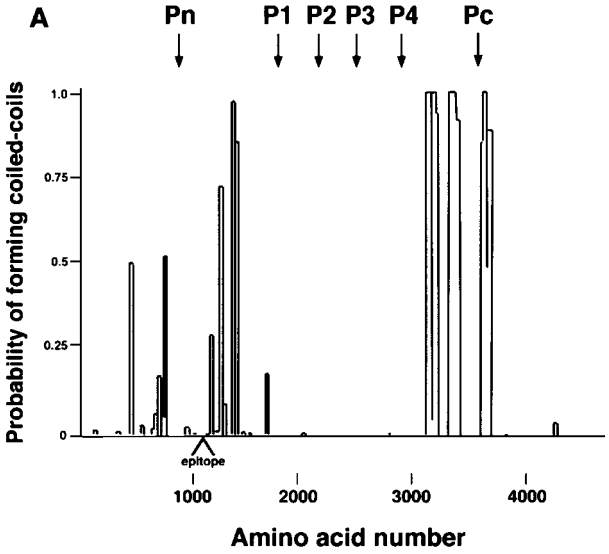

Figure 4. Secondary structure of the 1α Dhc. Shown here is a graphical representation of the regions of the 1α Dhc predicted to form α-helical coiled coils, as determined by the program COILS version 2.2 (Lupus et al., 1991; Lupus, 1996). The six regions of the sequence predicted to encode P-loops are identified by arrows. The position of the peptide sequence (amino acids 1,059-1,073) used to generate an isoform specific antibody (Myster et al., 1997) is also indicated.

lection. To confirm that the motility of the transformants was due to the successful expression of the *Dhc1* transgene and not a reversion event, two of the cW1 transformants (E2 and G4) were crossed with *oda2*, another mutant allele at the *PF28*/*ODA2* locus, and the progeny from 11 complete tetrads were analyzed for each cross. If the rescued motility was due to reversion of the *pf9-2* mutation, all the resulting tetrad progeny would be motile and swim with a *pf28*/*oda2*–like motility phenotype. However, if the rescued motility was due to the presence of the *Dhc1* transgene, then the restored motility phenotype would be expected to segregate independently of the *pf9-2* mutation, and a class of immotile progeny with the original *pf9-2 pf28* genotype should be recovered. Surprisingly, we observed three different motility phenotypes in the tetrad progeny. The first class swam with a motility phenotype that was indistinguishable from either *pf28* or *oda2*. The second class swam with a jerky motion like the *pf28*/*oda2* strains but appeared slower. The third class was immotile with short, stumpy flagella. The recovery of aflagellate strains demonstrated that the original *pf9-2* mutation was still present in the genetic background of the two transformants and that the rescued motility was due to the presence of the *Dhc1* transgene.

Motility Phenotypes of the Dhc1 Transformants

Although the frequency of rescue was low, it was clear that the rescued motility was due to the presence of the different *Dhc1* transgenes, and so the motility phenotypes of the *Dhc1* transformants were analyzed in greater detail. More specifically, we measured the flagellar beat frequency, the forward swimming velocity, and the ability to phototax (Table II). Transformants with complete rescue of the *pf9* mutation would be expected to have a swimming phenotype nearly identical to that of *pf28*. The flagellar beat frequencies of the *Dhc1* transformants were almost identical to the beat frequency of *pf28*, but measurements of forward swimming velocities clearly indicated that most of the transformants swam more slowly than *pf28* (Table II). In particular, the swimming velocities of the rescued strains obtained by transformation with the cosmid clones and pD1SA were slower than those obtained by transformation with the BAC clones. These results suggested that there were still some inner arm defects in most of the *Dhc1* transformants.

We next tested if the *Dhc1* transformants had recovered the ability to phototax. King and Dutcher (1997) have previously used a photoaccumulation assay to demonstrate that *pf9* mutant cells do not phototax effectively. Using similar conditions, we have found that *pf28* cells, which lack outer arms but have the full complement of inner dynein arms, are able to phototax, as assayed by their tendency to become concentrated in the illuminated portion of a tube within 40 min of exposure to a directional light source (Table II). However, all of the *Dhc1* transformants obtained with the cosmid clones remained equally distributed between the illuminated and darkened regions of the tube. To confirm these findings by direct observation of individual cells, the ability to phototax was also monitored in 96-well plates over a 60-min time course (see Materials and Methods). In the absence of outer arms, the *Dhc1* transformants obtained with the cosmid clones remained

Table II. Motility Phenotypes of Dhc1 Transformants

Strain name	*Dhc1* construct	Swimming velocity	Beat frequency	Ability to phototax
		μ/s, n ≥ 40	*Hz, n ≥ 20*	
pf28	N.A.	51.5 ± 6.9	21.8 ± 1.1	+
C1	cW1	37.8 ± 9.1	18.8 ± 0.9	−
E2	cW1	36.1 ± 5.5	18.7 ± 1.7	−
F2	cW1	42.4 ± 8.7	19.3 ± 0.7	−
F3	cW1	35.2 ± 5.4	18.9 ± 1.6	−
F4	cW1	36.5 ± 6.1	21.2 ± 1.4	−
F5	cW1	37.5 ± 7.0	20.2 ± 1.9	−
F7	cW1	37.0 ± 8.2	19.5 ± 1.1	−
G3	cW1	34.9 ± 5.7	21.0 ± 2.3	−
G4	cW1	41.2 ± 5.6	22.3 ± 2.1	−
G9	cW1	41.2 ± 9.9	20.3 ± 1.3	−
G11	cW1	41.1 ± 8.4	19.5 ± 1.5	−
H10	pD1SA	40.9 ± 9.2	19.7 ± 0.9	−
A2	cA1	29.6 ± 4.1	15.9 ± 1.3	−
2A-1B	N24-1	45.6 ± 7.7	N.D.	+
2B-4E	N24-1	46.4 ± 5.8	N.D.	+
4B-C2	J1-5	44.6 ± 6.0	N.D.	+
4B-G2	J1-5	45.4 ± 6.9	N.D.	+
5B-G10	J1-5	44.8 ± 4.1	N.D.	+
Outer arms present				
wild-type	N.A.	150.3 ± 20.3	61.1 ± 3.2	+
pf9-2	N.A.	73.4 ± 12.4	58.4 ± 3.1	−
pf9-3	N.A.	72.3 ± 14.1	60.8 ± 2.2	−
G4+OA	cW1	136.9 ± 16.5	57.4 ± 2.1	+
E2+OA	cW1	136.7 ± 10.5	61.4 ± 0.7	+

N.A., not applicable; ND, not determined.

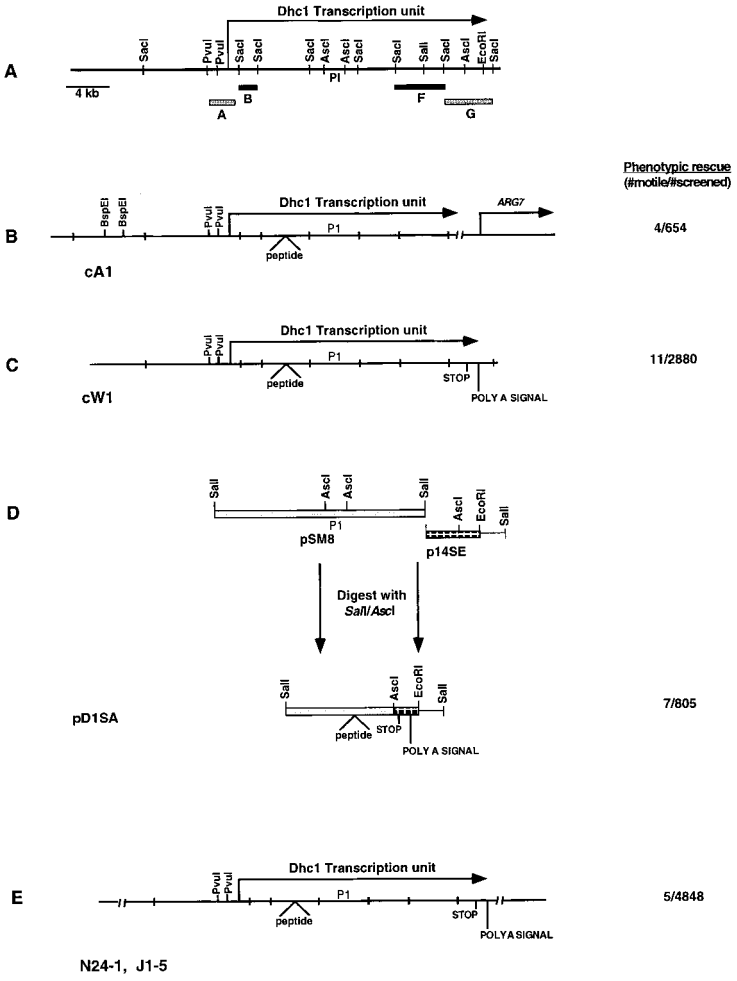

Figure 5. Constructs of the *Dhc1* gene used in the cotransformation experiments. (A) Partial restriction map of the *Dhc1* gene. The arrow above identifies the position of the *Dhc1* transcription unit within this region (Myster et al., 1997). SacI subclones (black and gray boxes) were used to screen two cosmid libraries to identify clones that contain the complete *Dhc1* transcription unit. (B) Partial restriction map of the cosmid cA1. The approximate locations of the regions encoding the primary ATP hydrolytic site (P1) and the peptide (peptide) recognized by the 1α Dhc specific antibody (Myster et al., 1997) are shown. The cA1 clone is incomplete on the 3′ end of the *Dhc1* gene; it encodes up to residue 4,105 of the 1α Dhc sequence followed by the addition of 87 novel amino acids. Before transformation, the cA1 cosmid was linearized with *Bsp*E1, leaving >8 kb of flanking genomic DNA upstream of the predicted translation start site. The *ARG7* sequence used as a selectable marker is located downstream of the *Dhc1* sequence. (C) Partial restriction map of the cosmid cW1 containing a full-length *Dhc1* gene. The regions encoding P1 and the peptide epitope are indicated, as are the predicted translation stop site (stop), and the consensus polyadenylation signal TGTAA (poly A signal). Before transformation, the cW1 cosmid was digested with *Pvu*I, which releases the *Dhc1* transcription unit as a 26-kb fragment flanked by ~1.6 kb of genomic DNA on the 5′ end and ~4 kb of genomic and vector DNA on the 3′ end. (D) Construction of a truncated version of the *Dhc1* gene. An 11-kb SalI-AscI fragment from pSM8 was subcloned into the SalI-AscI digested p14SE plasmid. The resulting pD1SA construct contains ~1.7 kb of genomic DNA 5′ of the predicted translation start site, the region encoding the first 1,956 amino acids, including the epitope recognized by the 1α Dhc antibody, and an ~1-kb fragment containing the 3′ end of the gene. The shift in the open reading frame after the AscI site results in the addition of nine novel amino acids (QCHGCGPGV) followed by a stop. This construct was linearized with SalI before transformation. (e) Recovery of BAC clones containing the *Dhc1* gene. Two different, large insert BAC clones were used in cotransformation experiments. The insert in the N24-1 clone contains ~18 kb upstream and ~52 kb downstream of the *Dhc1* gene, whereas the insert in J1-5 contains ~52 kb of genomic DNA both upstream and downstream of the *Dhc1* gene. These constructs were not linearized before transformation.

equally distributed in both the illuminated and darkened portions of the microtiter well. Conversely, the majority of *pf28* cells became concentrated on the illuminated side of the well within 15 min. These results indicated that this group of *Dhc1* transformants does not phototax as effectively as *pf28* control cells.

To examine the motility of the transformants in the presence of outer arms, two strains, G4 and E2, were crossed to *pf9-3* and tetrad products containing the *Dhc1* transgene in a wild-type outer arm background (G4+OA and E2+OA) were recovered. The two strains have beat frequencies almost identical to wild type, but their swimming velocities are intermediate in speed between *pf9* and wild type (Table II). Moreover, in the presence of the outer arms, the two strains could photoaccumulate as effectively as wild type. These results suggest that the outer arms can compensate in some way for the phototaxis defects in the *Dhc1* transformants.

Truncated 1α Dhcs in the Dhc1 Transformants

The swimming behavior of the *Dhc1* transformants obtained with the cosmid clones demonstrated that the introduction of these *Dhc1* clones resulted in only a partial rescue of the *pf9* motility defects. Given the large size of the *Dhc1* transcription unit (>22 kb), we were initially concerned that these transgenes might not be expressing wild-type levels of the *Dhc1* gene product. To address this question, we isolated axonemes from the *Dhc1* transformants and analyzed the components of the I1 complex. Previous work has shown that the I1 complex is composed of eight polypeptides, two Dhcs (1α and 1β), three ICs (IC140, IC138, and IC110) (Smith and Sale, 1991; Porter et al., 1992; Myster et al., 1997), and three LCs (LC8, LC12, and LC14) (Harrison et al., 1998). The *Dhc1* gene encodes the 1α Dhc, which can be identified on Western blots using antibody directed against a peptide epitope in the NH_2-ter-

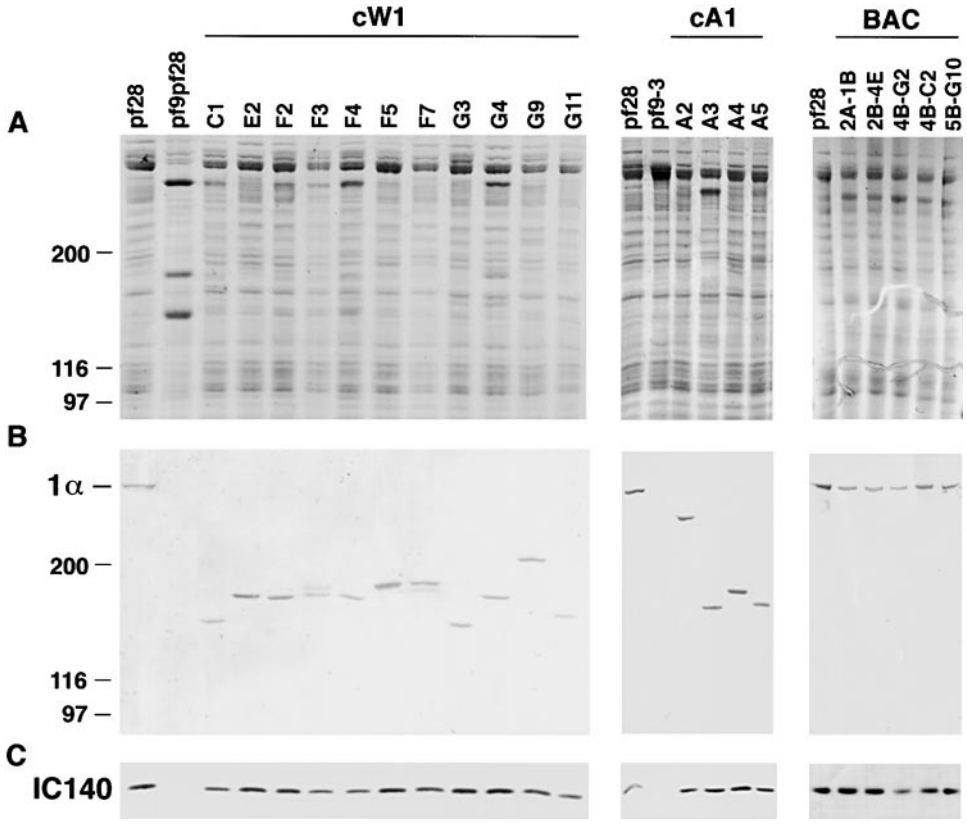

Figure 6. Western blots of isolated axonemes from *Dhc1* transformants. Isolated axonemes were prepared from the *Dhc1* transformants, split into triplicate for separation on 5% polyacrylamide gels, and then either stained with Coomassie blue or transferred to membranes and incubated with the affinity-purified 1α Dhc antisera or the IC140 antisera. (A, left panel) A 5% polyacrylamide gel loaded with 20-μg whole axonemes from *pf28*, *pf9 pf28*, and the 11 motile *Dhc1* transformants generated by transformation with the cW1 cosmid. The additional bands in the *pf9 pf28* sample are most likely contaminating flagellar membrane proteins. (Middle panel) A 5% gel loaded with whole axonemes from *pf28*, *pf9-3*, and the four rescued strains generated by transformation with the cA1 cosmid. (Right panel) A 5% gel loaded with whole axonemes from *pf28* and the five rescued strains obtained with the BAC clones. (B) Duplicate immunoblots probed with the affinity-purified 1α Dhc antibody. (C) Duplicate immunoblots probed with the IC140 antisera. Control blots probed with tubulin antibodies confirmed that roughly equivalent amounts of flagellar protein were loaded in each lane (data not shown).

minal region (Myster et al., 1997). Fig. 6 A shows three Coomassie blue–stained polyacrylamide gels containing whole axonemes isolated from several mutant strains: the 11 motile *Dhc1* transformants obtained with the cW1 cosmid, the 4 motile *Dhc1* transformants recovered with the cA1 construct, and the 5 transformants recovered with the *Dhc1* BAC clones. Fig. 6 B shows the corresponding Western blots probed with the 1α Dhc antibody. The 1α Dhc antibody identified the ~520 kD 1α Dhc in the *pf28* control sample, but polypeptides significantly smaller than the 1α Dhc were identified in all of the motile strains obtained by transformation with the *Dhc1* cosmids. In contrast, all of the axoneme samples prepared from rescued strains obtained by transformation with the *Dhc1* BAC clones contained full-length 1α Dhc polypeptides. These results indicated that the partial rescue phenotype seen with the *Dhc1* cosmid clones was not due to low levels of expression of a full-length 1α Dhc, but instead due to the expression of truncated 1α Dhcs, ranging in size from ~165 to ~300 kD.

To determine if other I1 subunits were associated with the truncated 1α Dhcs, Western blots of isolated axonemes were probed with an antiserum raised against the 140-kD intermediate chain (Yang and Sale, 1998). This antibody detects the IC140 in wild-type axonemes, but not in I1 mutant axonemes. As shown in Fig. 6 C, the IC140 antibody recognized a single polypeptide of ~140 kD in *pf28* and each rescued transformant, but did not detect the IC140 in any of the *pf9* mutant strains. Similar results were seen using the antibody directed against the 14-kD Tctex1 light chain (data not shown).

Assembly of I1 Complexes in Dhc1 Transformants

To confirm that the other polypeptide subunits were assembled into an I1 complex, we isolated whole axonemes from large-scale cultures of two *Dhc1* transformants, E2 and G4, as well as from control *pf28* cells. Partially purified I1 complexes were obtained by high salt extraction of the isolated axonemes followed by sucrose density gradient centrifugation. The resulting fractions were analyzed by both SDS-PAGE and Western blotting. Fig. 7 A shows the 19S region of a sucrose gradient that was loaded with the *pf28* dynein extract. The two Dhcs and three ICs of the I1 isoform cosediment as a complex that peaks in fraction number 4. Duplicate samples tested on Western blots probed with the 1α Dhc antibody confirmed the presence of the 1α Dhc in the 19S region (right). Fig. 7 B shows four fractions from the sucrose gradient that was loaded with the G4 dynein extract. The gel on the left reveals that the 1β Dhc and the three intermediate chains of the I1 complex have shifted and now cosediment at ~16S, peaking in fraction 6. A novel polypeptide of ~183 kD cosediments in the same region (see asterisks). Western blot analysis

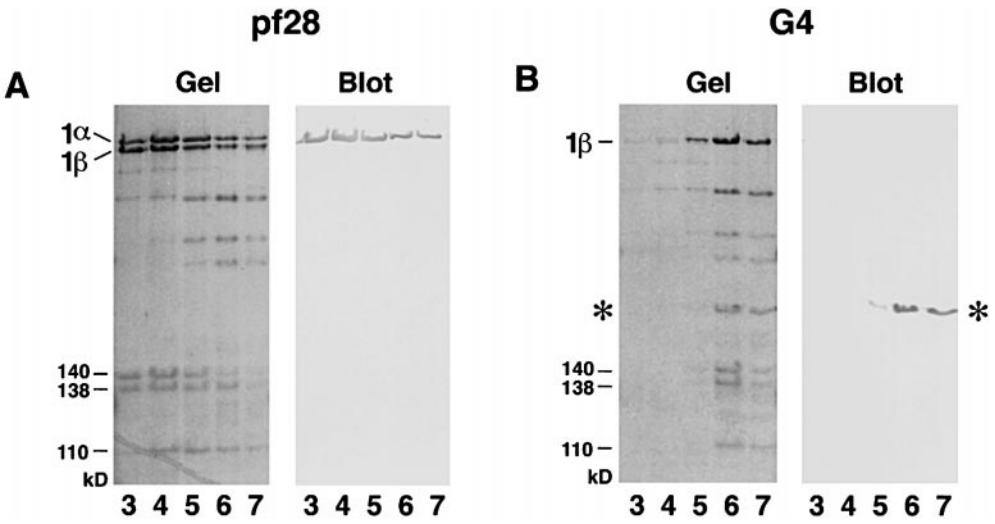

Figure 7. Cosedimentation of the truncated 1α Dhc with other subunits of the I1 complex. Whole axonemes were isolated from *pf28* and the *Dhc1* transformant G4 and extracted with high salt to release the dynein arms. The crude dynein extracts were loaded onto a 5–20% sucrose gradient and centrifuged for 15 h at 33,500 *g*. Duplicate samples from the 19S region of the gradients were separated on 5% polyacrylamide gels and either stained with Coomassie blue or transferred to nitrocellulose and incubated with the affinity-purified 1α Dhc antibody. (A) Gel and corresponding immunoblot from the *pf28* extract. (B) Gel and corresponding immunoblot from the G4 extract. The asterisk identifies the truncated 1α Dhc that cosediments at ~16S with the other subunits of the I1 complex.

with the 1α Dhc antibody identified this novel band as the truncated 1α Dhc (Fig. 7 B, blot). Identical results were observed with dynein extracts isolated from the E2 strain (data not shown). The truncated 1α Dhcs in the *Dhc1* transformants therefore form stable complexes with the other polypeptides of the I1 complex, but the resulting mutant complexes sediment more slowly than wild-type complexes.

Structural Analysis of Axonemes from Dhc1 Transformants Reveals Defects in the I1 Complex

To analyze the structure of the I1 complex in the *Dhc1* transformants, we prepared purified axonemes from wild-type and mutant strains for thin section EM. To facilitate the analysis of the images, the transformants G4 and E2 were crossed to a *pf9-3* strain to recover the *Dhc1* transgene in a wild-type outer arm background (G4+OA and E2+OA, see Materials and Methods). Fig. 8 a shows the grand average of the 96-nm repeat from wild-type axonemes, and Fig. 8 b indicates the corresponding densities. Previous work has shown that the inner dynein arms repeat as a complex group of structures every 96 nm in register with the radial spokes (Muto et al., 1991; Mastronarde et al., 1992). The I1 complex is a trilobed structure located proximal to the first radial spoke (S1) in each 96-nm repeat (Fig. 8 b, lobes 1–3) (Piperno et al., 1990; Mastronarde et al., 1992; Myster et al., 1997). These three lobes are missing in *pf9-3* axonemes (Fig. 8, c and d), which lack the I1 complex (Myster et al., 1997). Fig. 8, e and g, show the grand averages of the axonemes from the G4+OA and E2+OA strains, which contain I1 complexes with truncated 1α Dhcs. Lobes 1 and 3 of the I1 complex are present in the axonemes from these samples, but lobe 2 is still missing. Difference plots between these images and wild type confirms that the loss of lobe 2 is the only significant defect in the two *Dhc1* transformants (Fig. 8, f and h). These images demonstrate that the I1 complex is assembled and targeted to the appropriate axoneme location. In addition, these images suggest that the region of the 1α Dhc that is missing in the *Dhc1* transformants corresponds to lobe 2 of the I1 structure.

The Dhc1 Transcripts in the Cosmid Transformants Lack the 3′ End of the Gene

Although the initial cotransformation experiments involved the use of a full-length or near full-length *Dhc1* cosmid clones, all of the motile transformants recovered with these clones assemble partially functional I1 complexes with truncated 1α Dhcs (Fig. 6 and Table II). To understand how the 1α Dhc fragments were related to the *Dhc1* sequence, we analyzed the *Dhc1* transcripts from several of the rescued transformants on Northern blots. Total RNA was first isolated from the G4+OA and E2+OA strains, which contain the *Dhc1* transgene in the *pf9-3* null mutant background. This background facilitated our analysis because the *pf9-3* mutation is a large deletion (~13 kb) in the *Dhc1* gene and does not generate an endogenous *Dhc1* transcript (Myster et al., 1997).

Fig. 9 A shows a partial restriction enzyme map of the *Dhc1* gene and the subclones that were used as probes to analyze the *Dhc1* transcripts. As shown in Fig. 9 B, probe A3′, which spans the *Dhc1* transcription start site, identified a single, large (>13 kb) transcript in wild-type RNA. However, in G4+OA and E2+OA, the transcripts recognized by the A3′ probe were significantly smaller than the wild-type *Dhc1* transcript, but these smaller transcripts were still upregulated in response to deflagellation (compare lanes 0 and 45). Identical results were observed with the next two subclones, probes B and C. Probe D, which includes the conserved region encoding the primary ATP hydrolytic site, hybridized to the truncated transcripts in E2+OA, but it did not recognize the truncated transcripts in G4+OA. Probes E–G did not hybridize with any transcripts in the transformants (Fig. 9 B, right panel, and data

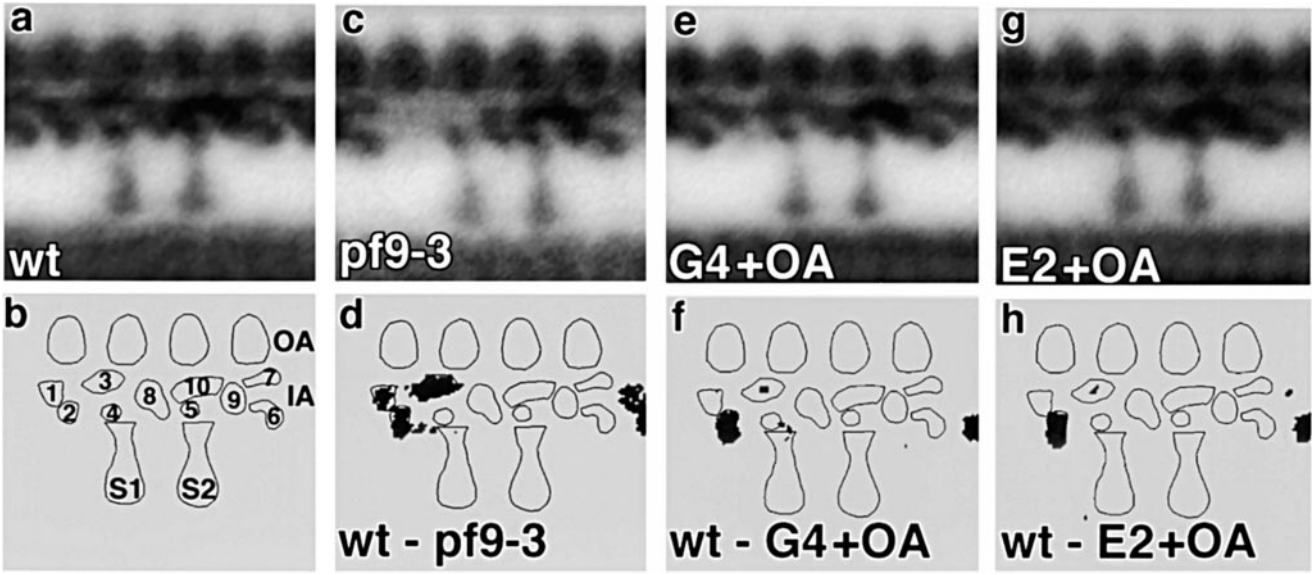

Figure 8. Structural defects in *Dhc1* transformants. Analysis of longitudinal images of axonemes from (a) wild-type, (c) *pf9-3*, (e) G4+OA, and (g) E2+OA. Grand averages for wild-type, *pf9-3*, G4+OA, and E2+OA based on 9, 6, 10, and 9 individual axonemes and 62, 44, 89, and 77 repeating units, respectively. (b) Outline of the individual densities in the 96-nm axonemal repeat. OA indicates positions of four outer dynein arm complexes per 96-nm repeat. S1 and S2 indicate the proximal and distal radial spokes, respectively. IA indicates the structures (numbered 1–10) seen in the inner arm region. (d) Difference plot between wild-type and *pf9-3*, with differences not significant at the 0.005 confidence level set to zero. (f) Difference plot between wild-type and G4+OA. (h) Difference plot between wild-type and E2+OA.

not shown). The *Dhc1* transcripts in G4 and E2 are therefore truncated from the 3′ end of the *Dhc1* gene, and G4 is truncated before E2.

To characterize the *Dhc1* transcripts present in other transformants, RNA was isolated from three additional strains: G3, G9, and A2. G3 and G9 are the cW1 transformants that assemble the smallest and largest 1α Dhc fragments respectively, whereas A2 is a cA1 transformant that

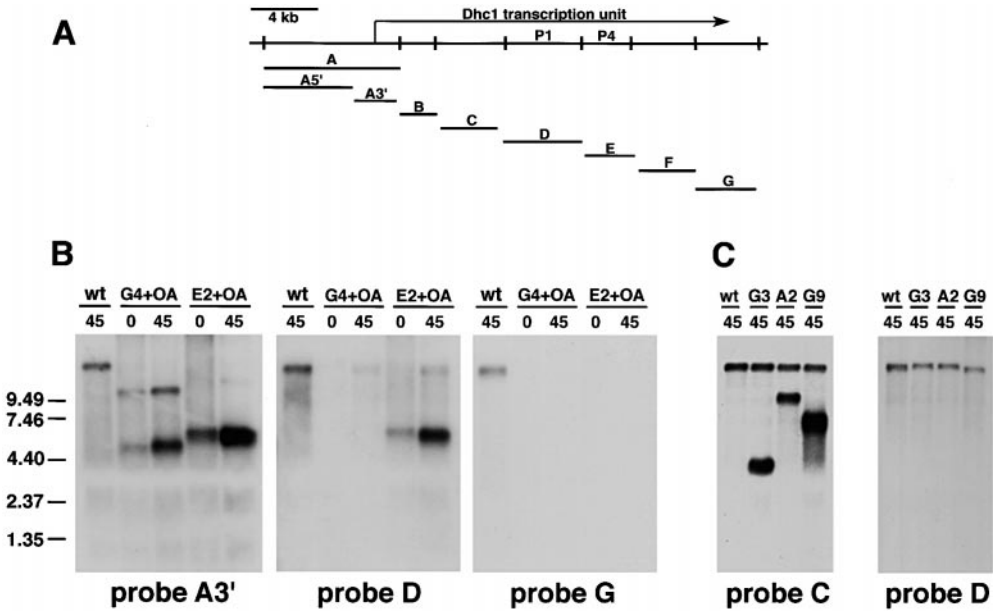

Figure 9. Northern blot analysis of *Dhc1* transcripts in rescued strains. (A) Partial restriction map of the *Dhc1* gene and subclones used as probes in the Northern analysis. (B) Northern blots of total RNA from wild-type, G4+OA, and E2+OA, isolated before (0) and 45 min (45) after deflagellation. Parallel samples of 20 μg total RNA were separated on 0.75% formaldehyde-agarose gels, transferred to Zetabind, and hybridized with selected *Dhc1* subclones. Each probe hybridized to a single, large (>14 kb) transcript in wild-type (wt). Probe A3′ (left panel) also hybridized to truncated *Dhc1* transcripts that are upregulated in response to deflagellation in G4+OA and E2+OA. Probes B and C gave similar results. Probe D (middle panel) hybridized to the truncated *Dhc1* transcript in E2+OA, but not in G4+OA. (Probe D, which corresponds to the most highly conserved region of the *Dhc1* gene, also cross-hybridized weakly with other *Dhc* transcripts in these samples.) Probe G (right panel) did not detect any transcripts in either G4+OA or E2+OA, and similar results were seen with probes E and F. (C) Northern blots of total RNA from wild-type, G3, A2, and G9 isolated 45 min (45) after deflagellation. Each probe hybridized to a single transcript in wild-type (wt) as well as the endogenous *Dhc1* transcript present in the *pf9-2* background of the transformants (Myster et al., 1997). Probe C (left panel) hybridized to the truncated *Dhc1* transcripts in G3, A2, and G9, but probes D–F (middle panel) did not.

assembles the largest (>300 kD) 1α Dhc fragment obtained thus far (Fig. 6). As shown in Fig. 9 C, in each strain, probe C hybridized to a truncated transcript that is significantly smaller than the endogenous *Dhc1* transcript derived from the *pf9-2* mutant background. However, probe D, which corresponds to the region encoding the ATP hydrolytic site, failed to hybridize with the truncated transcripts present in the G3, A2, and G9 samples. Similar results were seen with probes E and F (data not shown). Therefore, all three strains encode 1α Dhc fragments that are truncated before the proposed motor domain.

Recovery of a Modified Transgene from a Dhc1 Transformant

To identify the sites where the *Dhc1* cosmid clones were being modified during transformation, we isolated genomic DNA from the transformants and analyzed the structure of the integrated *Dhc1* transgenes on Southern blots. Fig. 10 A shows a blot of SacI digested genomic DNA that was hybridized with a probe for subclone C. As expected, this probe hybridized to the endogenous *Dhc1* gene present in the *pf9-2* mutant background of the transformants. However, for each transformant, a second polymorphic band could be detected using either probe C (Fig 10 A) or probe D (data not shown). From these and other blots, we concluded that the *Dhc1* cosmids were being rearranged during integration into genomic DNA. In addition, the region of the *Dhc1* gene encoding the conserved motor domain appeared to be the most common target for disruption during these integration events.

Because the G3 transformant assembles the smallest 1α Dhc fragment identified thus far (Fig. 6), we recovered the modified *Dhc1* transgene using probe C to screen a mini-library made from genomic DNA of the G3 transformant (see Materials and Methods). The *Dhc1* transgene was then sequenced with *Dhc1* specific primers to identify the junction between the *Dhc1* sequence and the site of integration in G3 genomic DNA. The *Dhc1* sequence in G3 is fused to an unidentified DNA sequence, and the resulting hybrid gene is predicted to encode up to amino acid residue 1,249 of the 1α Dhc, followed by the addition of 17 novel amino acids before encountering a stop codon (Fig. 10 B). Sequence analysis of an RT-PCR product derived from G3 RNA has confirmed the presence of this hybrid transcript. The polypeptide encoded by the modified transgene would, therefore, correspond to a 1α Dhc fragment of ~143 kD that is truncated just COOH-terminal to the epitope recognized by the 1α Dhc antibody (Fig. 10 C). The recovery of this fragment in G3 axonemes (Fig. 6) reveals that the NH_2-terminal coiled-coil domains of the 1α Dhc are not required for I1 complex assembly.

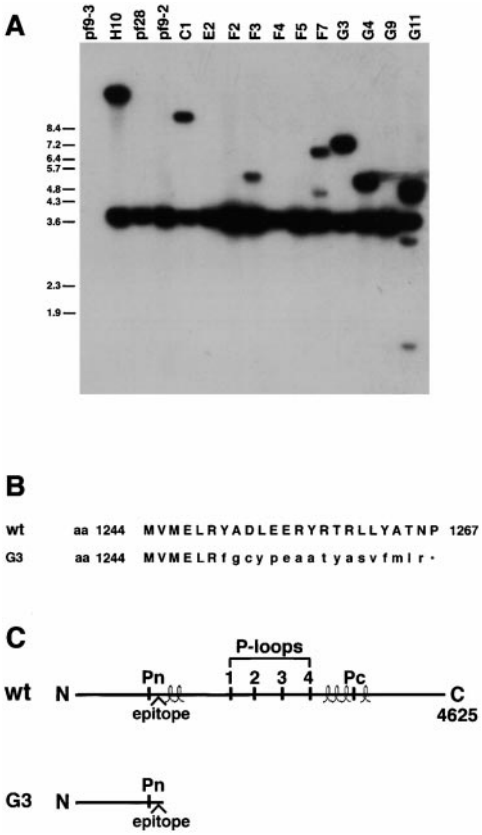

Figure 10. Modification of the *Dhc1* transgenes in the transformants. (A) Southern blot analysis of the *Dhc1* transgenes after integration into the *pf9-2 pf28* host strain. DNA was isolated from *pf9-3*, *pf28*, *pf9-2*, the H10 strain obtained by transformation with pD1SA, and the 11 rescued strains generated by transformation with cW1. 4 μg of genomic DNA was digested with SacI, separated on an 0.8% agarose gel, transferred to Magnagraph, and hybridized with probe C (Fig. 1). Probe C identifies the endogenous 4.2-kb SacI fragment in every sample except *pf9-3*, which contains a 13-kb deletion of the *Dhc1* gene (Myster et al., 1997). Probe C also hybridizes to novel restriction fragments in a subset of the transformants, which indicates that this region was a frequent site of rearrangement of the *Dhc1* transgenes. Rearrangements in the region corresponding to probe D were identified in the remaining samples (data not shown). (B) Determination of the predicted amino acid sequence of the 1α Dhc fragment in the G3 transformant. The truncated *Dhc1* transgene was recovered by screening a mini-library constructed from G3 genomic DNA (see Materials and Methods). The 3′ end of the transgene was sequenced with *Dhc1* specific primers. The nucleotide sequence revealed that the *Dhc1* transgene was fused to an unidentified DNA sequence. The resulting hybrid gene encodes up to residue 1,249 of the 1α Dhc, and then adds 17 novel amino acids before encountering a stop. (C) Schematic representation of the truncated 1α Dhc polypeptide present in transformant G3. The top line is the wild-type 1α Dhc showing the approximate positions of the P-loops, the predicted coiled-coil domains, and the peptide epitope recognized by the 1α Dhc antibody. Below is a similar diagram of the 1α Dhc fragment in G3. The sequence ends at amino acid 1,249, shortly after the epitope recognized by the 1α Dhc antibody.

Discussion

16 different *Dhc* genes have been identified in *Chlamydomonas*: 2 cytoplasmic *Dhc* sequences (Pazour et al., 1999; Porter et al., 1999), 3 genes that encode the Dhcs of the outer dynein arm (Mitchell and Brown, 1994, 1997; Wilkerson et al., 1994), and 11 other *Dhc* genes whose expression patterns are consistent with gene products that are involved in flagellar function (Porter et al., 1996, 1999;

Knott, J., and M. Porter, unpublished results). The analysis of specific Dhc mutations has revealed the role of each outer arm Dhc in flagellar motility (Sakakibara et al., 1991, 1993; Porter et al., 1994; Rupp et al., 1996), but the specific functions of the multiple inner arm Dhcs are largely unknown. We have previously demonstrated that the *Dhc1* gene product plays an essential role in the assembly and function of the I1 inner arm complex (Porter et al., 1996; Myster et al., 1997). To better understand how this inner arm Dhc contributes to flagellar motility, we have now analyzed the structure and function of the *Dhc1* gene and the encoded 1α Dhc in detail.

Sequence Analysis of Dhc1 Transcription Unit

As described in Fig. 1, we have determined the nucleotide sequence for the complete *Dhc1* transcription unit and used this information to obtain the predicted amino acid sequence of the 1α Dhc (Fig. 2). To our knowledge, this is the first full-length, inner arm Dhc sequence to be reported in any organism. Comparisons to other full-length Dhc sequences indicate that the 1α Dhc is most similar to the β and γ Dhcs of the outer arm, and that these sequence similarities extend into the NH_2-terminal region (Fig. 3). As the NH_2-terminal region of the Dhc is thought to be involved in the association with isoform specific IC and LC subunits, these observations suggest that the 1α Dhc and the β and γ Dhc contain conserved sites for the binding of accessory subunits. Indeed, recent studies have revealed that the I1 complex and the outer arm do contain similar IC and LC components, such as the 8-kD LC, the Tctex1 and Tctex2 LCs, and a family of WD-repeat containing ICs (Patel-King et al., 1997; Harrison et al., 1998; Yang and Sale, 1998). However, a novel feature of the 1α Dhc sequence is the presence of a P-loop motif (Pn) at amino acid residues 960–967 (Fig. 2). A weakly conserved P-loop motif has also been identified within the first 200 residues of the β Dhc (Mitchell and Brown, 1994; Kandl et al., 1995). Whether the Pn sequence in the 1α Dhc is a bona fide nucleotide binding site is unknown, but the future sequence analyses of 1α Dhc homologues in other organisms should indicate whether the Pn motif is a conserved feature of this class of Dhc.

The central and COOH-terminal thirds are the most highly conserved regions of the 1α Dhc, and our transformation experiments are consistent with previous proposals that this region corresponds to the dynein motor domain (Sakakibara et al., 1993; Koonce and Samso, 1996, Gee et al., 1997). The amino acid residues around P1 (the primary ATP hydrolytic site) and P4 are highly conserved with other axonemal Dhcs, whereas the sequences around P2 and P3 are less well conserved (Gibbons et al., 1994; Gibbons, 1995). For example, P3 does not strictly conform to the P-loop consensus sequence GXXXXGKS/T (Walker et al., 1982), as the glycine in position 6 is substituted by an alanine in the 1α Dhc sequence, but the same amino acid substitution was found in the γ Dhc sequence (Wilkerson et al., 1994).

The COOH-terminal third of the 1α Dhc also contains a small region ~340 amino acids downstream from P4 that is predicted to form a limited coiled-coil domain (Fig. 4). A similar region in cytoplasmic Dhc sequences has been identified recently as the stalk structure that extends from the globular head domain and forms the microtubule binding site (Koonce, 1997; Gee et al., 1997; Gee and Vallee, 1998). Mutations in this region in the outer arm β Dhc can have dramatic effects on flagellar motility (Porter et al., 1994). Interestingly, a sixth P-loop motif (Pc) has been identified in the 1α Dhc sequence, ~280 amino acids downstream from the proposed microtubule binding site. The function of this sixth P-loop in the 1α Dhc is unknown, but its position downstream from the microtubule binding site is intriguing. Recent sequence analysis has suggested that all dyneins may contain six ATPase-like repeat regions: the four central P-loops previously identified and two additional, less well conserved repeats after the COOH-terminal coiled-coil domains (Neuwald et al., 1999).

Rescue of the pf9 Mutant Phenotype by Transformation with Dhc1 Constructs

Using the *Dhc1* sequence information, we recovered two BAC clones and two cosmid clones containing full-length or near full-length *Dhc1* genes, and then used these constructs to rescue the *pf9* motility defects (Fig. 5). 20 independent transformants with rescued motility were recovered. Backcrossing the transformants confirmed that the rescued motility was due to the presence of the *Dhc1* transgene and not to a reversion event at the *PF9* locus. However, analysis of the *Dhc1* transformants produced two unexpected results. First, the frequency of rescue (<1%) was much lower than previously observed with other flagellar genes (5–10%) (Diener et al., 1990; Kindle, 1990; Tam and Lefebvre, 1993), and second, the 1α Dhcs were truncated in most of the motile transformants recovered thus far.

One reason that the cotransformation frequencies were so low might be due to the large size of the *Dhc1* transcription unit, which could make the *Dhc1* transgenes more susceptible to damage during the transformation protocol. Exogenous DNA sequences often undergo deletions as they integrate into the *Chlamydomonas* genome (Tam and Lefebvre, 1993; Smith and Lefebvre, 1996, 1997; Koutoulis et al., 1997). The recovery of truncated 1α Dhc fragments (Fig. 6) indicated that the *Dhc1* cosmids were being disrupted during the transformation protocol, and both Southern and Northern blot analyses of the rescued transformants (Fig. 9 and 10) have confirmed that deletions from the 3′ end of the *Dhc1* cosmids did occur. The presence of additional genomic DNA flanking the *Dhc1* transcription unit in the BAC clones may have served to protect the *Dhc1* transgenes and thereby permitted the full-length rescues observed with these clones (Figs. 5 and 6).

Another reason for the low frequency of rescue might be the relatively small amount of genomic DNA present on the 5′ end of the *Dhc1* gene in certain constructs (Fig. 5). If this region was randomly deleted, the resulting cotransformants would not retain the sequences necessary for expression of the *Dhc1* transcript and rescue of the mutant phenotype. Recent experiments with constructs encoding the IC140 subunit have indicated that sufficient DNA upstream from the 5′ end of the IC140 gene is essen-

tial for efficient rescue of the *ida7* mutation (Perrone et al., 1998).

The NH_2-terminal 143-kD of the 1α Dhc Is Sufficient for Complex Assembly

The second unexpected result was the frequency with which we recovered motile transformants expressing only NH_2-terminal fragments of the 1α Dhc (Fig. 6 B). Northern and Southern blot analyses have shown that the rescued strains retained the 5′ sequence elements required for regulated expression of the *Dhc1* transcripts, but several of these strains lacked the 3′ end of the transgene (Figs. 9 and 10). Therefore, the truncated 1α Dhcs represent those NH_2-terminal fragments that were competent to assemble with other subunits into the I1 complex (Fig. 6, B and C, and Fig. 7).

The observation that none of the 1α Dhc fragments is smaller than ~143 kD may indicate that this is the shortest NH_2-terminal fragment capable of complex assembly. Studies of outer arm mutants have identified a novel β Dhc mutation with similar properties. The *oda4-s7* mutant expresses a 160-kD fragment of the β Dhc that is capable of coassembly with other outer arm subunits at the correct axoneme location (Sakakibara et al., 1993). Likewise, low level expression of cytoplasmic Dhc constructs in *Dictyostelium* indicates that a 158-kD NH_2-terminal fragment is also capable of complex assembly (Koonce and Knecht, 1998).

Although the NH_2-terminal third of the 1α Dhc is the most variable region, secondary structure programs have identified a region just before P1 that is predicted to form a limited coiled-coil domain (Fig. 4). This domain, which has been identified in nearly all Dhcs sequenced to date (Mitchell and Brown, 1994, 1997), has been proposed as a potential region that might mediate interactions between the Dhcs and their associated ICs and LCs. To determine if this coiled-coil domain is required for assembly of the I1 complex, we recovered the *Dhc1* transgene from the G3 transformant, which expresses the shortest 1α Dhc fragment (Fig. 6 B). Sequence analysis of the truncated *Dhc1* transgene demonstrated that the 1α Dhc sequence terminates before the region predicted to form the NH_2-terminal coiled-coil domain (Fig. 10). Given that this 1α Dhc fragment still assembles with other I1 components into the flagellar axoneme (Fig. 6), other sites within the NH_2-terminal region must be required for complex formation. We plan to analyze additional *Dhc1* constructs to further delineate the domains required for specific subunit interactions and complex assembly.

Assembly of the Dynein Motor Domain

If the *Dhc1* transgenes were deleted randomly from the 3′ end, we would expect to recover a broad distribution of Dhc fragments ranging in size from the minimum required to assemble the I1 complex to nearly full-length. Therefore, why are almost all of the 1α Dhc fragments smaller than ~217 kD (Fig. 6 B)? One possibility may be that larger 1α Dhc fragments are unstable and prevent assembly of the I1 complex into the axoneme. Studies in *Dictyostelium* have shown that constructs of cytoplasmic Dhc lacking significant portions of the COOH terminus are expressed poorly as compared with other constructs that contain the entire motor domain (Koonce, 1997). Alternatively, the presence of larger 1α Dhc fragments with partial motor domains may inhibit flagellar motility. If so, we would not recover such transformants in our screen, which was based on the rescue of a motility defect. Indeed, Northern blot analysis of the two transformants (A2 and G9) that assemble the largest 1α Dhc fragments demonstrates that the sequences encoding the dynein motor domain are not present in the associated *Dhc1* transcripts (Fig. 9). The NH_2-terminal regions of these larger 1α Dhc fragments must, therefore, be fused to other protein sequences. Interestingly, the absence of motile transformants with partial motor domains is consistent with previous reports that nucleotide binding by the cytoplasmic Dhc is inhibited by deletion of the COOH terminus, leading to the formation of rigor complexes (Gee et al., 1997).

Implications for the Structure of the I1 Complex

Structural studies of the isolated I1 complex by negative staining or rotary shadowing have shown that it is a two-headed isoform (Goodenough et al., 1987; Smith and Sale, 1991) but the physical relationship between the globular heads seen in vitro and the structural domains identified in situ has been unknown. Because some of the *Dhc1* transformants assemble I1 complexes that lack central and COOH-terminal regions of the 1α Dhc (Fig. 7), we can now identify the position of the 1α motor domain within the I1 structure. EM analysis of axonemes isolated from the E2 and G4 transformants has revealed that lobe 2 of the I1 structure corresponds to the missing 1α motor domain (Fig. 8). Lobe 2 is close to the first radial spoke, in a position that may permit direct signaling between the radial spoke and the 1α Dhc motor domain. We predict that the remaining two lobes of the I1 structure represent the positions of the 1β Dhc motor domain and stem region containing the I1 ICs and LCs respectively. We are currently transforming other I1 mutants with the genes for other I1 subunits to identify the polypeptide components that are located within these structural domains (Perrone et al., 1998; Perrone, C.A., E. O'Toole, and M.E. Porter, work in progress).

The Role of the 1α Dhc Motor Domain in Motility and Phototaxis

The recovery of transformants missing only the 1α Dhc motor domain but containing the other components of the I1 complex has allowed us to analyze the specific role of the 1α Dhc motor domain in flagellar motility. I1 mutants lacking both the 1α and 1β Dhcs have a slow, smooth swimming phenotype with an altered flagellar waveform (Kamiya et al., 1991; Porter et al., 1992). Measurements of swimming velocities reveal that the *Dhc1* transformants with truncated 1α Dhcs swim faster than I1 mutants but slower than control strains containing both Dhcs (Table II). The 1α Dhc motor domain, therefore, contributes directly to force production during motility.

The I1 complex is also an essential component of the phototaxis response in *Chlamydomonas*. Strains that have defects in outer dynein arms, the dynein regulatory complex, or other inner arm isoforms can phototax, but mu-

tants lacking the I1 complex cannot (King and Dutcher, 1997). Analysis of other phototaxis mutants that retain the I1 complex reveals that the phosphorylation state of IC138 is altered (King and Dutcher, 1997). In vitro sliding assays have shown that the phosphorylation state of the IC138 affects microtubule sliding velocities (Habermacher and Sale, 1997). These results suggest a model in which the phosphorylation state of the IC138 modulates the activity of the I1 Dhc motor domains.

To assess the specific role of the 1α Dhc motor domain in phototaxis, we compared the swimming behavior of the *Dhc1* transformants to that of control cells in response to a directional light source. *pf28* cells were clearly phototactic, but the *Dhc1* transformants with truncated 1α Dhcs remained uniformly dispersed during the time course of our assays. These observations indicate that the motor activity of the 1α Dhc contributes to phototaxis, at least in the absence of the outer arms. However, if the outer arms were present, the *Dhc1* transformant strains could undergo phototaxis, whereas I1 mutant strains could not (Table II). This difference in behavior in the presence or absence of outer arms suggests that there are cooperative interactions between the I1 complex and the outer arms during the phototaxis response.

Previous studies have demonstrated that differences in the activity of the cis and trans flagellum are the basis of the phototaxis response (Kamiya and Witman, 1984; Rüffer and Nultsch, 1991, 1997; Horst and Witman, 1993; Witman, 1993). This differential activity includes both differences in beat frequency between the two flagella as well as differences in flagellar waveforms (Sakakibara and Kamiya, 1989; Rüffer and Nultsch, 1991). The outer dynein arms are responsible for generating the differences in beat frequency observed between cis and trans flagella, as the cis-trans frequency differential is lost in mutants that lack the outer arm or the outer arm α Dhc (Sakakibara and Kamiya, 1989; Sakakibara et al., 1991). More recent work has demonstrated that this differential beat frequency depends on the presence of the docking structure that facilitates the attachment of the outer arm to its specific binding site on the A-tubule (Takada and Kamiya, 1997). The differential in beat frequency is not essential for the phototaxis response (Rüffer and Nultsch, 1991), as outer arm mutant cells such as *pf28* are capable of phototaxis (Table II). However, it is clear that the cis-trans differences in beat frequency and flagellar waveform must be coupled in some way, because phototaxis mutants such as *ptx1* are defective in both (Rüffer and Nultsch, 1997; Takada and Kamiya, 1997). In this context, it appears that regulation of the I1 complex is important for generating the asymmetries in flagellar waveform between the cis and trans flagella that contribute to phototaxis (King and Dutcher, 1997), whereas regulation of the outer arm contributes to the differential in flagellar beat frequency (Takada and Kamiya, 1997). Phototaxis can occur in the absence of the outer arms, but not the I1 complex (King and Dutcher, 1997; Table II). However, if both the outer arms and part of the I1 complex are present (such as in G4+OA or E2+OA), then their combined activity can apparently compensate for the absence of the 1α Dhc motor domain.

These observations raise several interesting questions about the mechanism by which changes in the phosphorylation state of IC138 might contribute to phototaxis. For example, where is IC138 located in the axoneme relative to the motor domains of the two I1 Dhcs and the three outer arm Dhcs? Is it in lobe 3 of the I1 structure, which is also in close proximity to at least one outer arm per axoneme repeat? Does IC138 interact directly with either the 1α or 1β Dhc? We are planning to address these questions by analyzing subunit interactions within the I1 complex. Other important questions concern the identity and location of the axonemal kinases and phosphatases that modulate the phosphorylation state of IC138. Work from other laboratories has indicated that many of these regulatory components are tightly bound to the flagellar axoneme (Habermacher and Sale, 1997; King and Dutcher, 1997; Yang, P., and W.S. Sale. 1998. The M_r 140,000 intermediate chain of *Chlamydomonas* flagellar inner arm dynein is a WD-repeat containing protein implicated in dynein arm anchoring. *Mol. Biol. Cell.* 9:3335–3349), but the specific enzymes that act on either the outer arm or the I1 IC138 in situ have not yet been identified. The future identification and localization of these regulatory components will provide new insights into the pathway that governs the activity of the multiple dynein motors during flagellar motility and phototaxis.

We wish to thank other members of the Porter laboratory for their advice and support during the course of this project. We are also grateful to the members of the laboratories of C. Silflow, P. Lefebvre, and R. Linck (University of Minnesota) for their helpful suggestions at our weekly group meetings. Parts of this work were completed by S.H. Myster in partial fulfillment of the requirements for a Ph.D. degree at the University of Minnesota.

This work was supported by a grant from the National Institutes of General Medical Sciences (GM 55667) to M.E. Porter and S.H. Myster was supported in part by a research training grant from the National Science Foundation for Interdisciplinary Studies on the Cytoskeleton (DIR91134444). E. O'Toole was supported by a National Institutes of Health Biotechnology Resource (RR00592) grant to J.R. McIntosh.

Submitted: 27 May 1999
Revised: 19 July 1999
Accepted: 20 July 1999

References

Brokaw, C.J., and R. Kamiya. 1987. Bending patterns of *Chlamydomonas* flagella IV. Mutants with defects in inner and outer dynein arms indicate differences in dynein arm function. *Cell Motil. Cytoskeleton.* 8:68–75.

Debuchy, R., S. Purton, and J.-D. Rochaix. 1989. The argininosuccinate lyase gene of *Chlamydomonas reinhardtii*: an important tool for nuclear transformation and for correlating the genetic and molecular maps of the *ARG7* locus. *EMBO (Eur. Mol. Biol. Organ.) J.* 8:2803–2809.

Diener, D.R., A.M. Curry, K.A. Johnson, B.D. Williams, P.A. Lefebvre, K.L. Kindle, and J.L. Rosenbaum. 1990. Rescue of paralyzed-flagella mutant of *Chlamydomonas* by transformation. *Proc. Natl. Acad. Sci. USA.* 87:5739–5743.

Eversole, R.A. 1956. Biochemical mutants of *Chlamydomonas reinhardtii*. *J. Bot.* 43:404–407.

Gardner, L.C., E. O'Toole, C.A. Perrone, T. Giddings, and M.E. Porter. Components of a dynein regulatory complex are located at the junction between the radial spokes and the dynein arms in *Chlamydomonas* flagella. *J. Cell Biol.* 127:1311–1325.

Gee, M., and R. Vallee. 1998. The role of the dynein stalk in cytoplasmic and flagellar motility. *Eur. Biophys. J.* 27:466–473.

Gee, M.A., J.E. Heuser, and R.B. Vallee. 1997. An extended microtubule-binding structure within the dynein motor domain. *Nature.* 390:636–639.

Gibbons, I.R. 1995. Dynein family of motor proteins: present status and future questions. *Cell Motil. Cytoskeleton.* 32:136–144.

Gibbons, B.H., D.J. Asai, W.-J.Y. Tang, T.S. Hays, and I.R. Gibbons. 1994. Phylogeny and expression of axonemal and cytoplasmic dynein genes in sea urchins. *Mol. Biol. Cell.* 5:57–70.

Goodenough, U.W., B. Gebhart, V. Mermall, D.R. Mitchell, and J.E. Heuser.

1987. High pressure liquid chromatography fractionation of *Chlamydomonas* dynein extracts and characterization of inner arm dynein subunits. *J. Mol. Biol.* 194:481–494.

Habermacher, G., and W.S. Sale. 1997. Regulation of flagellar dynein by phosphorylation of a 138-kD inner arm dynein intermediate chain. *J. Cell Biol.* 136:167–176.

Harris, E. 1989. The *Chlamydomonas* sourcebook. Academic Press, Inc., San Diego, CA. 780 pp.

Harrison, A., and S.M. King. 1999. The molecular anatomy of dynein. *Essays Biochem*. 35:In press.

Harrison, A., P. Olds-Clarke, and S.M. King. 1998. Identification of the *t* complex-encoded cytoplasmic dynein light chain Tctex1 in inner arm I1 supports the involvement of flagellar dyneins in meiotic drive. *J. Cell Biol.* 140:1137–1147.

Horst, C., and G. Witman, 1993. *ptx1*, a nonphototactic mutant of *Chlamydomonas*, lacks control of flagellar dominance. *J. Cell Biol.* 120:733–741.

Kagami, O., and R. Kamiya. 1992. Translocation and rotation of microtubules caused by multiple species of *Chlamydomonas* inner-arm dynein. *J. Cell Sci.* 103:653–664.

Kamiya, R. 1988. Mutations at twelve independent loci result in absence of outer dynein arms in *Chlamydomonas reinhardtii*. *J. Cell Biol.* 107:2253–2258.

Kamiya, R., E. Kurimoto, and E. Muto. 1991. Two types of *Chlamydomonas* flagellar mutants missing different components of inner arm dynein. *J. Cell Biol.* 112:441–447.

Kamiya, R. and G. Witman. 1984. Submicromolar levels of calcium control the balance of beating between the two flagella in demembranated models of *Chlamydomonas. J. Cell Biol.* 98:97–107.

Kandl, K.A., J.D. Forney, and D.J. Asai. 1995. The dynein genes of *Paramecium tetraurelia*: the structure and expression of the ciliary β and cytoplasmic heavy chains. *Mol. Biol. Cell*. 6:1549–1562.

Kindle, K.L. 1990. High-frequency nuclear transformation of *Chlamydomonas reinhardtii*. *Proc. Natl. Acad. Sci. USA*. 87:1228–1232.

King, S.J., and S.K. Dutcher. 1997. Phosphoregulation of an inner dynein arm complex in *Chlamydomonas reinhardtii* is altered in phototactic mutant strains. *J. Cell Biol.* 136:177–191.

King, S.J., W.B. Inward, E.T. O'Toole, J. Power, and S.K. Dutcher. 1994. The *bop2-1* mutation reveals radial asymmetry in the inner dynein arm region of *Chlamydomonas reinhardtii*. *J. Cell Biol.* 126:1255–1266.

King, S.M., T. Otter, G.B. Witman. 1986. Purification and characterization of *Chlamydomonas* flagellar dyneins. *Meth. Enzymol.* 134:291–306.

King, S.M., C.G. Wilkerson, and G.B. Witman. 1991. The M_r 78,000 intermediate chain of *Chlamydomonas* outer arm dynein interacts with α-tubulin *in situ*. *J. Biol. Chem*. 266:8401–8407.

King, S.M., R.S. Patel-King, C.G. Wilkerson, and G.B. Witman. 1995. The 78,000-M_r intermediate chain of *Chlamydomonas* outer arm dynein is a microtubule-binding protein. *J. Cell Biol.* 131:399–409.

King, S.M., E. Barbarese, J.F.I. Dillman, R.S. Patel-King, J.H. Carson, and K.K. Pfister. 1996. Brain cytoplasmic and flagellar outer arm dynein share a highly conserved M_r 8,000 light chain. *J. Biol. Chem*. 271:19356–19366.

Koonce, M.P. 1997. Identification of a microtubule-binding domain in a cytoplasmic dynein heavy chain. *J. Biol. Chem*. 272:19714–19718.

Koonce, M.P., and M. Samso. 1996. Overexpression of dynein's globular head causes a collapse of the interphase microtubule network in *Dictyostelium*. *Mol. Biol. Cell* 7:935–948.

Koonce, M.P., and D.A. Knecht. 1998. Cytoplasmic dynein heavy chain is an essential gene product in *Dictyostelium*. *Cell Motil. Cytoskeleton*. 39:63–77.

Koonce, M.P., P.M. Grissom, and J.R. McIntosh. 1992. Dynein from *Dictyostelium*: primary structure comparisons between a cytoplasmic motor enzyme and flagellar dynein. *J. Cell Biol.* 119:1597–1604.

Koutoulis, A., G.J. Pazour, C.G. Wilkerson, K. Inaba, H. Sheng, S. Takada, and G.B. Witman. 1997. The *Chlamydomonas reinhardtii ODA3* gene encodes a protein of the outer dynein arm docking complex. *J. Cell Biol.* 137:1069–1080.

Laemmli, U.K. 1970. Cleavage of structural proteins during the assembly of the head of bacteriophage T4. *Nature*. 227:680–685.

LeDizet, M., and G. Piperno. 1995. *ida4-1*, *ida4-2*, and *ida4-3* are intron splicing mutations affecting the locus encoding p28, a light chain of *Chlamydomonas* axonemal inner dynein arms. *Mol. Biol. Cell*. 6:713–723.

Levine, R.P., and W.T. Ebersold. 1960. The genetics and cytology of *Chlamydomonas. Annu Rev. Microbiol.* 14:197–216.

Lupus, A. 1996. Prediction and analysis of coiled coil structures. *Methods. Enzymol*. 266:513–525.

Lupus, A., M. Van Dyke, and J. Stock. 1991. Predicting coiled coils from protein sequences. *Science*. 252:1162–1164.

Mastronarde, D.N., E.T. O'Toole, K.L. McDonald, J.R. McIntosh, and M.E. Porter. 1992. Arrangement of inner dynein arms in wild-type and mutant flagella of *Chlamydomonas*. *J. Cell Biol.* 118:1145–1162.

Mitchell, D.R. 1994. Cell and molecular biology of flagellar dyneins. *Int. Rev. Cyt.* 155:141–175.

Mitchell, D.R., and J.L. Rosenbaum. 1985. A motile *Chlamydomonas* flagellar mutant that lacks outer dynein arms. *J. Cell Biol.* 100:1228–1234.

Mitchell, D.R., and J.L. Rosenbaum. 1986. Protein-protein interactions in the 18S ATPase of *Chlamydomonas* outer dynein arms. *Cell Motil. Cytoskeleton*. 6:510–520.

Mitchell, D.R., and Y. Kang. 1991. Identification of *oda6* as a *Chlamydomonas* dynein mutant by rescue with the wild-type gene. *J. Cell Biol.* 113:835–842.

Mitchell, D.R., and K.S. Brown. 1994. Sequence analysis of the *Chlamydomonas* α and β dynein heavy chain genes. *J. Cell Sci.* 107:635–644.

Mitchell, D.R., and K.S. Brown. 1997. Sequence analysis of the *Chlamydomonas reinhardtii* flagellar α dynein gene. *Cell Motil. Cytoskeleton*. 37:120–126.

Muto, E., R. Kamiya, and S. Tsukita. 1991. Double-rowed organization of inner dynein arms in *Chlamydomonas* flagella revealed by tilt series, thin-section electron microscopy. *J. Cell Sci.* 99:57–66.

Myster, S.H., J.A. Knott, E. O'Toole, and M.E. Porter. 1997. The *Chlamydomonas Dhc1* gene encodes a dynein heavy chain subunit required for assembly of the I1 inner arm complex. *Mol Biol. Cell*. 8:607–620.

Nakamura, Y., T. Gojobori, and T. Ikemura. 1997. Codon usage tabulated from the international DNA sequence databases. *Nucleic Acids Res.* 25:244–245.

Nelson, J.A.E., P.B. Savereide, and P.A. Lefebvre. 1994. The *Cry1* gene in *Chlamydomonas reinhardtii*: structure and use as a dominant selectable marker for nuclear transformation. *Mol. Cell. Biol.* 14:4011–4019.

Neuwald, A.F., L. Aravind, J.L. Spouge, and E.V. Koonin. 1999. AAA^+: A class of chaperone–like ATPases associated with the assembly, operation, and disassembly of protein complexes. *Genome Res.* 9:27–43.

Newman, S.M., J.E. Boynton, N.W. Gillham, B.W. Randolph-Anderson, A.M. Johnson, and E.H. Harris. 1990. Transformation of the chloroplast ribosomal RNA genes in *Chlamydomonas*: molecular and genetic characterization of integration events. *Genetics*. 126:875–888.

Patel-King, R.S., S.E. Benashski, A. Harrison, and S.M. King. 1997. A *Chlamydomonas* homologue of the putative murine *t* complex distorter Tctex-2 is an outer arm dynein light chain. *J. Cell Biol.* 137:1081–1090.

Pazour, G.J., B. Dickert, and G.B. Witman. 1999. The DHC1b (DHC2) isoform of cytoplasmic dynein is required for flagellar assembly. *J. Cell Biol.* 144: 473–481.

Perrone, C.A., P. Yang, E. O'Toole, W.S. Sale, and M.E. Porter. 1998. The *Chlamydomonas IDA7* locus encodes a 140 kDa dynein intermediate chain required to assemble the I1 inner arm complex. *Mol. Biol. Cell*. 9:3351–3365.

Piperno, G., and Z. Ramanis. 1991. The proximal portion of *Chlamydomonas* flagella contains a distinct set of inner dynein arms. *J. Cell Biol.* 112:701–709.

Piperno, G., Z. Ramanis, E.F. Smith, and W.S. Sale. 1990. Three distinct inner dynein arms in *Chlamydomonas* flagella: molecular composition and location in the axoneme. *J. Cell Biol.* 110:379–389.

Porter, M.E. 1996. Axonemal dyneins: assembly, organization, and regulation. *Curr. Opin. Cell Biol.* 8:10–17.

Porter, M.E., J. Power, and S.K. Dutcher. 1992. Extragenic suppressors of paralyzed flagellar mutations in *Chlamydomonas reinhardtii* identify loci that alter the inner dynein arms. *J. Cell Biol.* 118:1163–1176.

Porter, M.E., J.A. Knott, L.C. Gardner, D.R. Mitchell, and S.K. Dutcher. 1994. Mutations in the SUP-PF-1 locus of *Chlamydomonas reinhardtii* identify a regulatory domain in the β-dynein heavy chain. *J. Cell Biol.* 126:1495–1507.

Porter, M.E., J.A. Knott, S.H. Myster, and S.J. Farlow. 1996. The dynein gene family in *Chlamydomonas reinhardtii. Genetics*. 144:569–585.

Porter, M.E., R. Bower, J.A. Knott, P. Byrd, and W. Dentler. 1999. Cytoplasmic dynein heavy chain 1b is required for flagellar assembly in *Chlamydomonas. Mol. Biol. Cell*. 10:693–712.

Purton, S., and J.D. Rochaix. 1994. Complementation of a *Chlamydomonas reinhardtii* mutant using a genomic cosmid library. *Plant Mol. Biol.* 24:533–537.

Rüffer, U., and W. Nultsch. 1991. Flagellar photoresponses of *Chlamydomonas* cells held on micropipettes: II. Change in flagellar beat pattern. *Cell Motil. Cytoskeleton*. 18:269–278.

Rüffer, U., and W. Nultsch. 1997. Flagellar photoresponses of *ptx1*, a nonphototactic mutant of *Chlamydomonas*. *Cell Motil. Cytoskeleton*. 37:111–119.

Rupp, G., E. O'Toole, L.C. Gardner, B.F. Mitchell, and M.E. Porter. 1996. The *sup-pf-2* mutations of *Chlamydomonas* alter the activity of the outer dynein arms by modification of the γ-dynein heavy chain. *J. Cell Biol.* 135:1853–1865.

Sakakibara, H., and R. Kamiya. 1989. Functional recombination of outer dynein arms with outer arm-missing flagellar axonemes of a *Chlamydomonas* mutant. *J. Cell Sci.* 92:77–83.

Sakakibara, H., D.R. Mitchell, and R. Kamiya. 1991. A *Chlamydomonas* outer arm dynein mutant missing the α heavy chain. *J. Cell Biol.* 113:615–622.

Sakakibara, H., S. Takada, S.S.M. King, G.B. Witman, and R. Kamiya. 1993. A *Chlamydomonas* outer arm dynein mutant with a truncated β heavy chain. *J. Cell. Biol.* 122:653–661.

Sambrook, J., E.F. Fritsch, and T. Maniatis. 1989. Molecular Cloning: A Laboratory Manual. 2nd edition. Cold Spring Harbor Laboratory Press, Cold Spring Harbor, New York. 1.33–1.44 pp.

Smith, E.F., and W.S. Sale. 1991. Microtubule binding and translocation by inner dynein arm subtype I1. *Cell Motil. Cytoskeleton*. 18:258–268.

Smith, E.F., and P.A. Lefebvre. 1996. The *PF*16 gene product contains armadillo repeats and localizes to a single microtubule of the central apparatus in *Chlamydomonas* flagella. *J. Cell Biol.* 132:359–370.

Smith, E.F., and P.A. Lefebvre. 1997. *PF20* gene product contains WD repeats and localizes to the intermicrotubule bridges in *Chlamydomonas* flagella. *Mol. Biol. Cell*. 8:455–467.

Takada, S., and R. Kamiya. 1997. Beat frequency difference between the two flagella of *Chlamydomonas* depends on the attachment site of outer dynein arms on the outer-doublet microtubules. *Cell Motil. Cytoskeleton*. 36:68–75.

Tam, L.W., and P.A. Lefebvre. 1993. Cloning of flagellar genes in *Chlamy-*

domonas reinhardtii by DNA insertional mutagenesis. *Genetics.* 135:375–384.
Walker, J.E., M. Saraste, M.J. Runswick, and N.J. Gay. 1982. Distantly related sequences in the α- and β-subunits of ATP synthase myosin, kinases and other ATP-requiring enzymes and a common nucleotide binding fold. *EMBO (Eur. Mol. Biol. Organ.) J.* 1:945–951.
Wilkerson, C.G., S.M. King, and G.B. Witman. 1994. Molecular analysis of the γ heavy chain of *Chlamydomonas* flagellar outer arm dynein. *J. Cell Sci.* 107: 497–506.
Witman, G.B. 1986. Isolation of *Chlamydomonas* flagella and flagellar axonemes. *Methods Enzymol.* 134:280–290.
Witman, G.B. 1993. *Chlamydomonas* phototaxis. *Trends Cell Biol.* 3:403–408.
Witman, G.B., C.G. Wilkerson, and S.J. King. 1994. The Biochemistry, Genetics, and Molecular Biology of Flagellar Dynein. *In* Microtubules. J.S. Hyams and C.W. LLoyd, editors. Wiley-Liss, Inc., New York. 229–249.
Yang, P., L. Fox, and W.S. Sale. 1998. Characterization of an axonemal type-1 phosphatase that regulates flagellar dynein activity. *Mol. Biol. Cell.* 9:130a
Zhang, D. 1996. Regulation of nitrate assimilation in *Chlamydomonas reinhardtii.* Ph.D. Thesis, University of Minnesota.
Zhang, H., P.L. Herman, and D.P. Weeks. 1994. Gene isolation through genomic complementation using and indexed library of *Chlamydomonas reinhardtii* DNA. *Plant Mol. Biol.* 24:663–672.